THE BELL SYSTEM
TECHNICAL JOURNAL

VOLUME XXXVII MAY 1958 NUMBER 3

Distribution of the Duration of Fades in Radio Transmission:

Gaussian Noise Model

By S. O. RICE

(Manuscript received November 29, 1957)

The fluctuations of a received radio signal due to fading are assumed to behave like the envelope of narrow-band Gaussian noise. Estimates of the distribution of the fade lengths for various depths of fades are given, and relations which may be useful in analyzing fading data are derived. A similar problem involving the separation of the intercepts of the noise current itself, instead of its envelope, is also discussed.

I. INTRODUCTION

When a radio transmitter sends out a steady sine wave of very high frequency the signal received far beyond the horizon is no longer steady. The envelope of the received signal fluctuates in an irregular manner and may go through several maxima and minima in a second. These fluctuations have been studied by many people.* For observations extending over fifteen minutes or so, the variations in the size of the envelope follow, approximately, a Rayleigh distribution. For observations extending over a month, the distribution of the hourly medians is roughly normal in decibels with a standard deviation of 8 or 10 db. There are also seasonal and diurnal variations.

* In this paper we shall make use of the data given by K. Bullington, W. J. Inkster and A. L. Durkee.[1]

Here we shall be concerned mostly with the short-term Rayleigh fading. In particular we shall be interested in the distribution of the lengths of fades, i.e., in the lengths of the intervals during which the signal remains below some specified level — the lower the level, the "deeper" the fade.

We shall assume, in our calculations, that the envelope of the received wave is the same as the envelope of a Gaussian random noise current having a narrow, normal-law power spectrum centered on the transmitter frequency.* Under suitable conditions the distribution of the fade lengths approaches a limiting form for deep fades and the exact form of the power spectrum becomes unimportant.

Although the results obtained from the Gaussian noise model do not always agree with the rather meager available experimental data, they do show general trends. Moreover, a process of averaging over the parameters given in Section IV suggests relations between the depths of fades and their durations which may be of use in analyzing fading data.

Our method of studying the duration of fades may be described as follows. We first find an expression which approximates the distribution function in the region of short intervals. This is done by using the method developed in Section 3.4 of Ref. 2 for dealing with the intervals between the zeros of a random noise current. The second step is concerned with the very long intervals. Although it seems to be generally accepted that the probability of a fade exceeding a great length T decreases as $\exp(-\alpha T)$, no convenient method of calculating the exact value of α is available as yet. Here we more or less ignore this difficulty by using a method which amounts to plotting, on suitable coordinates, our approximation for short intervals and then extrapolating by eye so as to obtain a "reasonable" looking curve. This method is described in Section VI. It turns out that the slope of the extrapolated curve at the origin gives the value of α. Needless to say, the reader should regard these portions (the long fade portions) of our distribution curves merely as estimates.

In Section II we state some known results regarding the frequency and average duration of fades based on the Gaussian noise model. Section III lists the main results obtained in the later sections. In Section IV some of the results set forth in Section III are applied to radio fading problems and comparisons with experimental data are given. Section V is concerned with the lengths of the intervals during which a

* This power spectrum is obtained when the propagation is assumed to result from randomly moving scatterers having a Maxwellian distribution of velocities. Even if the power spectrum is not normal most of our formulas will still hold, but some of our curves will no longer apply.

Gaussian noise current $I(t)$ exceeds some given value I. Although the material in Section V is not directly related to the fading of the envelope, it is of interest in its own right and serves to set the stage for the work of Section VII, which deals with the intervals during which the envelope $R(t)$ of $I(t)$ lies below some given value R. A discussion of the computations is given in Section VIII. Several known results concerning the separation of the zeros of a simple Markoff process are listed in Section IX and their relation to the present work is pointed out.

II. THE AVERAGE DURATION OF A FADE

Here we shall state several known results regarding the fluctuation of a Gaussian noise current $I(t)$ and its envelope $R(t)$.* Let the mean square value of $I(t)$ be b (b is the same as ψ_0 and b_0 of Refs. 2 and 3). Then

$$\text{probability } I(t) > I \;=\; \tfrac{1}{2}[1 - P(Ib^{-1/2})], \tag{1}$$

$$\text{probability } R(t) > R = e^{-R^2/2b}, \tag{2}$$

where $P(x)$ is the error integral

$$P(x) = \frac{2}{\sqrt{2\pi}} \int_0^x e^{-t^2/2}\, dt. \tag{3}$$

Let $w(f)$ be the power spectrum of $I(t)$ and β be the $-\psi_0''$ of Ref. 2 so that

$$\beta = \int_0^\infty w(f)(2\pi f)^2\, df. \tag{4}$$

Then, according to a result due to Mark Kac, the expected number of times per second $I(t)$ passes upward across the level $I(t) = I$ is

$$N_I = \frac{1}{2\pi} (\beta/b)^{1/2} e^{-I^2/2b}. \tag{5}$$

The average length of the intervals during which $I(t) > I$ is the quotient of (1) and (5):

$$\begin{aligned} \bar{t} &= \pi(b/\beta)^{1/2} e^{I^2/2b}[1 - P(Ib^{-1/2})], & \\ \bar{t} &\sim \frac{b}{I}(2\pi/\beta)^{1/2}, & I \gg b^{1/2} \\ \bar{t} &\sim 2\pi(b/\beta)^{1/2} e^{I^2/2b}, & I \ll -b^{1/2} \end{aligned} \tag{6}$$

* See Refs. 2 and 3, where reference is made to the earlier work of V. D. Landon, K. A. Norton and others.

where the first asymptotic value follows from

$$\tfrac{1}{2}[1 - P(x)] \sim \frac{e^{-x^2/2}}{x\sqrt{2\pi}}, \qquad x \gg 1. \quad (7)$$

The corresponding results for the envelope run as follows.* Let $w(f)$ be confined to a narrow band and be symmetrical about the midband frequency f_0, and let β_r be the b_2 of Ref. 3 so that

$$\beta_r = 4\pi^2 \int_0^\infty w(f)(f - f_0)^2 \, df. \quad (8)$$

Then the expected number of times per second $R(t)$ passes downward across the level R is

$$N_R = (\beta_r/2\pi)^{1/2}(R/b)e^{-R^2/2b}. \quad (9)$$

The average length of the intervals during which $R(t) < R$ is, from (2) and (9),

$$\bar{t} = (b/R)\,(2\pi/\beta_r)^{1/2}(e^{R^2/2b} - 1). \quad (10)$$

When R becomes small

$$\bar{t} \to (R/2)\,(2\pi/\beta_r)^{1/2}. \quad (11)$$

In most of the following work we shall set b equal to 1 so that

$$\overline{I^2(t)} = b = \int_0^\infty w(f)\, df = 1. \quad (12)$$

When this is done we have

$$\begin{aligned} \bar{t}/\bar{t}_0 &= [1 - P(I)] \exp(I^2/2), \\ N_I/N_0 &= \exp(-I^2/2), \end{aligned} \quad (13)$$

where N_0 denotes the average number of upward crossings, per second, across the axis $I(t) = 0$ and $\bar{t}_0$ the average separation of the zeros of $I(t)$. Table I gives values of these ratios. They do not depend upon the power spectrum $w(f)$.

The ratios corresponding to (13) for $R(t)$ are

$$\begin{aligned} \bar{t}/\bar{t}_1 &= (e^{R^2/2} - 1)/R(e^{1/2} - 1) \approx 1.54\,(e^{R^2/2} - 1)/R, \\ N_R/N_1 &= R \exp[(1 - R^2)/2] \approx 1.649\, Re^{-R^2/2}, \end{aligned} \quad (14)$$

* K. A. Norton and his colleagues[4] have considered more general fading problems in which the received wave contains both a steady sinusoidal component and a Rayleigh-distributed component.

TABLE I — AVERAGE DURATIONS AND CROSSING RATES — $I(t)$

$I/\text{rms } I(t)$	$\bar{t}/\bar{t}_0$	N_I/N_0	$N_I\bar{t}$
-5	536,674	3.73×10^{-6}	$1 - 2.87 \times 10^{-7}$
-4	5,962	3.35×10^{-4}	0.999968
-3	180	0.0111	0.9986
-2	14.4	0.135	0.977
-1	2.77	0.607	0.841
0	1.000	1.000	0.500
1	0.523	0.607	0.159
2	0.336	0.135	0.0228
3	0.243	0.0111	0.00135
4	0.189	3.35×10^{-4}	3.17×10^{-5}
5	0.154	3.73×10^{-6}	2.87×10^{-7}

where $\bar{t}_1$ and N_1 refer to the level $R = 1$. Other reference levels sometimes used are

$$\begin{aligned} \text{median } R &= (2 \log 2)^{1/2} = 1.1774 \cdots \approx 1.18, \\ \text{average } R &= (\pi/2)^{1/2} \approx 1.25, \\ \text{rms } R &= 2^{1/2} \approx 1.41. \end{aligned} \tag{15}$$

Thus, instead of the second of equations (14), it is sometimes convenient to use

$$\frac{N_R}{N_m} = \frac{2R}{R_m} e^{-R^2/2} = \frac{2R}{R_m} \left(\frac{1}{2}\right)^{R^2/R_m^2},$$

where N_m and R_m refer to the median level. In (14) and (15) the value of b is unity, i.e., rms $I(t) = 1$, $I(t)$ being the noise current whose envelope is $R(t)$. Table II gives values of the ratios (14). Just as in the case of $I(t)$, these ratios do not depend on the power spectrum.

TABLE II — AVERAGE DURATIONS AND CROSSING RATES — $R(t)$

$R/\text{rms } I(t)$	$\bar{t}/\bar{t}_1$	N_R/N_1	$N_R\bar{t}$
0.125	0.0967	0.2045	0.00778
0.25	0.1957	0.3995	0.0308
0.5	0.4105	0.7275	0.1175
1.0	1.000	1.000	0.3935
1.18 (median)	1.309	0.9731	0.5000
2.0	4.924	0.4462	0.8647
3.0	45.74	0.0550	0.9889
4.0	1148	0.002212	0.999665

III. GAUSSIAN NOISE RESULTS — NORMAL-LAW POWER SPECTRUM

Let $I(t)$ be a Gaussian noise current with the power spectrum

$$w(f) = \frac{2}{\sigma\sqrt{2\pi}} e^{-f^2/2\sigma^2} \tag{16}$$

so that the mean square value of $I(t)$ is $b = 1$. When $I(t)$ crosses upward through the level I the probability that it will remain above I for more than τ seconds may be denoted by $F(u, I)$. Here

$$\begin{aligned} u &= \tau/\bar{t}, \\ \bar{t} &= (2\sigma)^{-1}[1 - P(I)] \exp(I^2/2), \\ \beta &= (2\pi\sigma)^2, \end{aligned} \tag{17}$$

where $\bar{t}$ is the average length obtained from (6).

Fig. 1 shows our estimates of $F(u, I)$ plotted against u for various values of I. These curves were obtained by the calculations described in Section VIII. As mentioned in the Introduction, the values of $F(u, I)$ for the larger values of u must be regarded as conjectures. Two special cases are

$$\begin{aligned} F(u, I \to -\infty) &= e^{-u}, \\ F(u, I \to \infty) &= e^{-u^2\pi/4}, \end{aligned} \tag{18}$$

and these hold not only for (16) but apparently for any power spectrum such that $F(u, I)$ exists. The gradual change of $F(u, I)$ from an exponential form to a Rayleigh form as I runs from $-\infty$ to $+\infty$ [as indicated by (18)] was surmised by D. S. Palmer[5] from an examination of some experimental data.*

A case which has received some attention in the literature occurs when

$$w(f) = 8/[1 + (2\pi f)^2]^2. \tag{19}$$

This power spectrum is unusual because it represents a borderline case between a simple Markoff process, for which $F(u, I)$ does not exist, and the smoother noise processes, one of which is represented by the $w(f)$ of (16). An experimental investigation of the spacings between zeros of $I(t)$ when $w(f)$ has the form (19) [and also when $w(f)$ has several similar forms] has been carried out by R. R. Favreau, H. Low and I. Pfeffer.[6]

* Mr. Palmer has informed me that the "Note added in proof" appearing in his paper should be disregarded. He has obtained a proof that the Rayleigh form is indeed approached at $I = \infty$. His proof is given in our Section V under the discussion of equation (66).

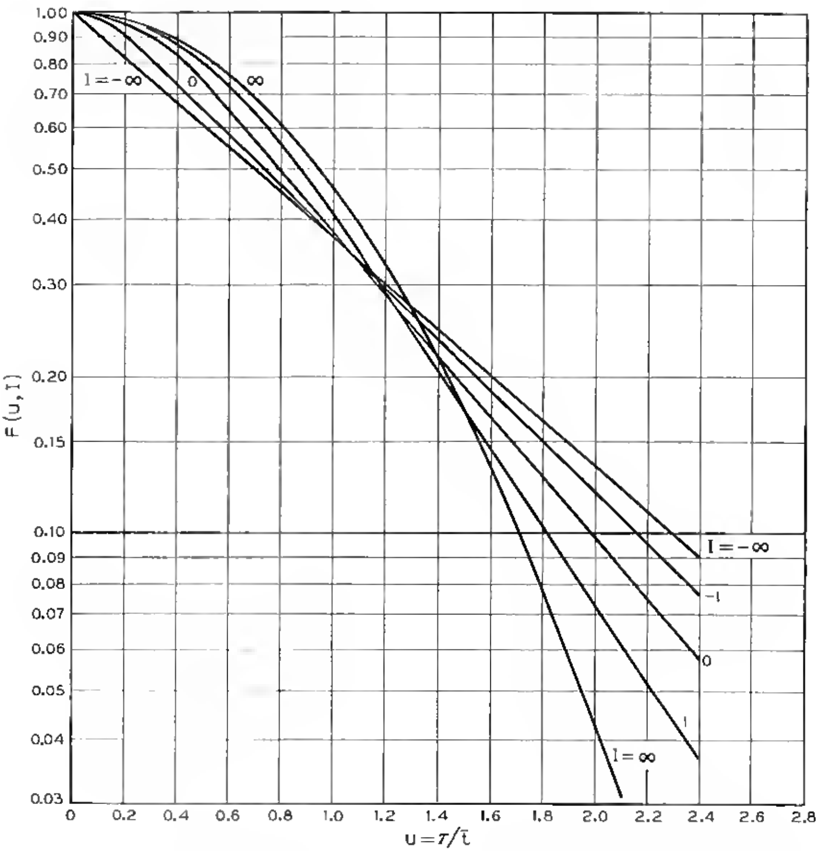

Fig. 1 — The probability $F(u, I)$ that $I(t) > I$ for an interval lasting longer than τ. $I(t)$ has a Gaussian power spectrum and $\bar{t}$ is given by equation (17).

D. S. Palmer[5] has obtained an approximate integral equation for the probability density $f(u, 0) = -\partial F(u, 0)/\partial u$ which has been improved by J. A. McFadden.[7] McFadden gives curves obtained by solving his equation numerically. They agree well with the experimental results of Ref. 6. For (19), $f(u, 0)$ appears to approach a value close to 1.25 as u approaches zero, whereas for (16), $f(u, 0)$ approaches zero.

The corresponding results for the envelope $R(t)$ may be stated as follows. Let $I(t)$ be a Gaussian noise current with the envelope $R(t)$ and the narrow-band power spectrum

$$w(f) = \sigma^{-1}(2\pi)^{-1/2} \exp\left[-(f - f_0)^2/2\sigma^2\right]. \tag{20}$$

When $R(t)$ crosses downward through the level R, the probability that it will remain below R for more than τ seconds may be denoted by $F_\tau(u, R)$, where now

$$\begin{aligned} u &= \tau/\bar{t}, \qquad \beta_r = (2\pi\sigma)^2, \\ \bar{t} &= (R\sigma)^{-1}(2\pi)^{-1/2}(e^{R^2/2} - 1), \end{aligned} \tag{21}$$

and $\bar{t}$ is computed from (10).

Estimates of $F_\tau(u, R)$ are given in Table III and the calculation of these values is discussed in Section VIII. Just as for $I(t)$, the values for the larger u's must be regarded as conjectures. The special cases corresponding to (18) are

$$F_\tau(u, R \to \infty) = e^{-u}, \tag{22}$$

$$F_\tau(u, R \to 0) = (2/u)I_1(2/\pi u^2) \exp(-2/\pi u^2), \tag{23}$$

where $I_1(z)$ denotes a Bessel function of imaginary argument. Again these limiting forms do not depend on $w(f)$. The values given in Table III are plotted in Fig. 2. It may be shown from (23) that, for small values of u, $F_\tau(u, R \to 0)$ is approximately $1 - \frac{3}{16}\pi u^2$ and, for large values of u, it decreases like $2/\pi u^3$. Since the $\bar{t}$ in the u of (23) is given by (11), u is proportional to τ/R, and hence $F_\tau(u, R \to 0)$ depends on τ and R only

TABLE III — ESTIMATES OF $F_\tau(u, R)$ FOR THE NARROW-BAND, NORMAL-LAW POWER SPECTRUM (20)

u	$R = 0$	$R = 0.5$	$R = 1$	$R = 1.18$	$R = 2$	$R = \infty$
0	1.00	1.00	1.00	1.00	1.00	1.00
0.1	0.995	0.994	0.993	0.992	0.976	0.905
0.2	0.976	0.974	0.969	0.963	0.885	0.819
0.3	0.945	0.938	0.924	0.906	0.793	0.741
0.4	0.894	0.884	0.843	0.808	0.711	0.670
0.5	0.823	0.804	0.733	0.694	0.637	0.606
0.6	0.729	0.697	0.624	0.598	0.571	0.549
0.7	0.619	0.588	0.535	0.528	0.511	0.496
0.8	0.521	0.492	0.464	0.467	0.458	0.449
0.9	0.429	0.412	0.407	0.413	0.411	0.406
1.0	0.354	0.343	0.360	0.364	0.368	0.368
1.2	0.242	0.249	0.279	0.285	0.296	0.301
1.4	0.171	0.190	0.216	0.222	0.237	0.246
1.6	0.122	0.149	0.168	0.174	0.190	0.202
1.8	0.0890	0.116	0.130	0.135	0.153	0.165
2.0	0.0681	0.0899	0.101	0.106	0.123	0.135
2.2	0.0535	0.0701	0.0784	0.0826	0.0987	0.111
2.4	0.0425	0.0544	0.0608	0.0645	0.0792	0.0907
2.6	0.0340	0.0421	0.0472	0.0504	0.0636	0.0743
2.8	0.0269	0.0327	0.0366	0.0393	0.0510	0.0608
3.0	0.0220	0.0253	0.0284	0.0307	0.0410	0.0498

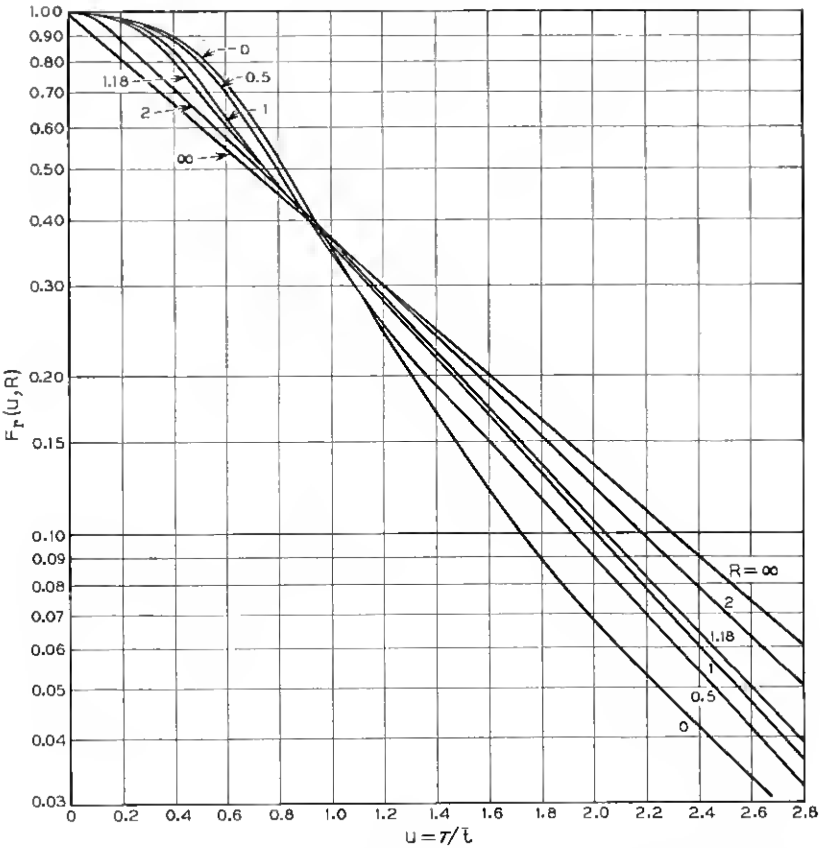

Fig. 2 — The probability $F_r(u, R)$ that $R(t) < R$ for an interval lasting longer than τ. $R(t)$ is the envelope of narrow-band Gaussian noise having the power spectrum (20).

through the ratio τ/R. The curves for $F_r(u, R \to 0)$ and $F_r(u, R \to \infty)$ cross near $u = 5.68$, where they both have the value 0.00340. This behavior is shown in Fig. 4.

IV. COMPARISON OF THEORY WITH EXPERIMENT

By combining the average fade lengths given by Table II and the fade length distributions $F_r(u, R)$ given by Table III, we obtain Fig. 3. In Fig. 3 the scales have been chosen so that the median value of $R(t)$ is 1.18 [see equations (15)], and so that fades below the median last one second, on the average. This leads to $\bar{t}_1 = 0.763$ seconds and $\beta_r = 4.53$

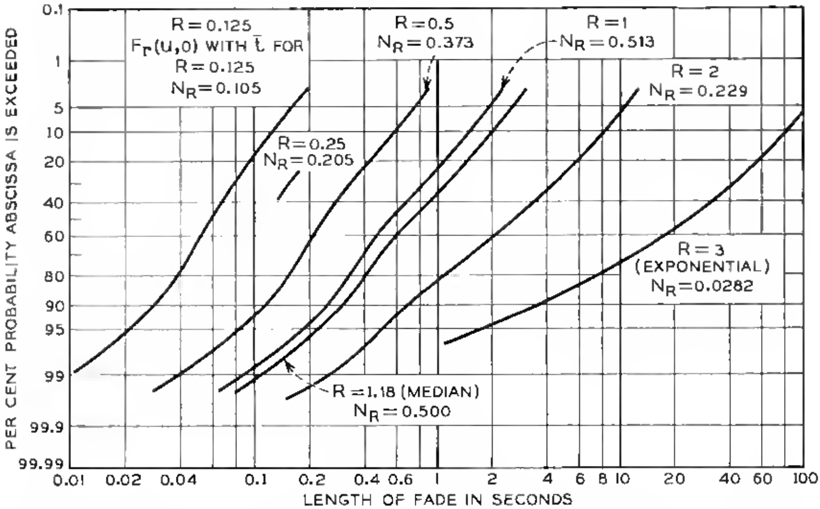

Fig. 3 — Distribution of the duration of fades. $R(t)$ is the envelope of narrow-band noise. The time scale is chosen so that fades below the median value of $R(t)$ have an average length of one second.

and makes $\sigma = 0.339$ in the associated power spectrum (20). When both R and τ/R are small, the ordinates of the curves on Fig. 3 are given approximately by $1 - 1.7(\tau/R)^2$. As R increases, the distribution changes from the form shown by (23) to the exponential (22).

When the available experimental results for rapid fading are studied, it is found that some of them seem to agree with Fig. 3, but others do not. It is not hard to find reasons for lack of agreement when it does occur. One is that we have arbitrarily taken the normal-law power spectrum (20) for our calculations. This gives fade length distributions $F_r(u, R)$ of the sort shown in Fig. 2. These distributions appear to be typical of those obtained for $w(f)$'s which (i) decrease rapidly for frequencies outside the nominal band and (ii) do not become excessively large for frequencies near f_0 (such frequencies correspond to slow fluctuations in the envelope). For $w(f)$'s which do not satisfy these requirements, say one which behaves like

$$w(f) = \frac{2k}{k^2 + 4\pi^2(f - f_0)^2} \tag{24}$$

when f is near f_0, k being very small, the work in Appendix IV suggests that the distribution curves have the quite different shape shown in Fig. 13. When the experimental curves differ from those of Fig. 2, they tend to look like those of Fig. 13.

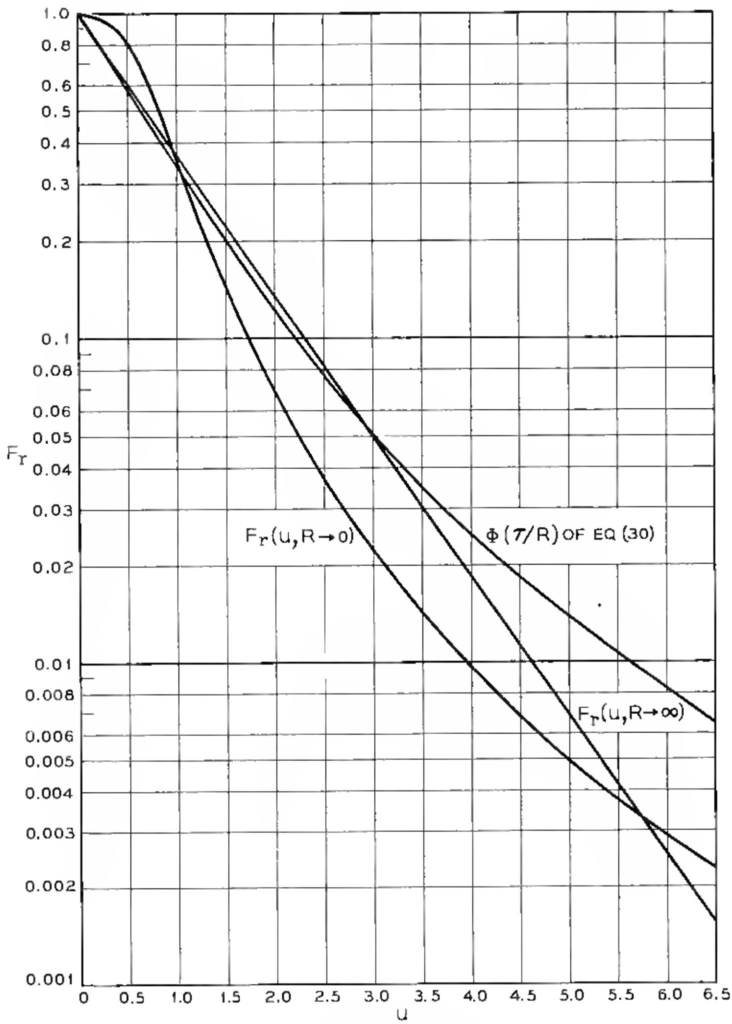

Fig. 4 — Plots of $F_r(u, R)$ for special cases. $F_r(u, R \to \infty)$ is given by (22). $F_r(u, R \to 0)$ corresponds to fixed values of the median and fading rate, and is given by (23). $\Phi(\tau/R)$ of (30) corresponds to fixed median but variable fading rate.

A second reason for the lack of agreement is that Fig. 3 refers to fixed values of the parameters b and β_r where $b^{1/2}$ is a measure of the median value ($R_m = 1.18b^{1/2}$) and $(\beta_r/b)^{1/2}$ is a measure of the rate of fluctuation [the average number of times $R(t)$ passes down across the median value in one second is $N_{R_m} = 0.235(\beta_r/b)^{1/2}$]. Actually, assuming

the Gaussian noise model to be valid, the values of b and β_r may change slowly during an experimental run. When the fluctuation is regarded as due to the Doppler effect of moving scatterers, $(\beta_r/b)^{1/2}$ is proportional to the average speed of the scatterers, which we might expect to be roughly proportional to the wind velocity in the scattering region. The value of b is the average received power and is proportional to the number of scatterers and to the average power scattered to the receiver by each. According to this picture, it is not surprising that β_r and b may change during an experimental run.

In spite of all of these uncertainties we shall attempt (perhaps rashly) to draw some conclusions from our formulas in the case of deep fades (R near zero). In this case a few of our formulas take a relatively simple form, and we may average over values of b and β_r or otherwise use the formulas as a guide. The reader should bear in mind that the statements in the remainder of this section are tentative and future experimentation may show them to be in error.

As an example of the averaging process, let us consider the expected number of times per second, N_R, the envelope of the received wave crosses downward across the value of R microvolts where R is very small. When we assume b and β_r to have the joint probability density $g(b, \beta_r)$ and take the average of expression (9) (with R so small that the exponential term is almost unity), we find that if $g(b, \beta_r)$ satisfies suitable conditions,

$$\begin{aligned} N_R &\approx R \int_0^\infty \int_0^\infty b^{-1}(\beta_r/2\pi)^{1/2}\, g(b, \beta_r)\, db\, d\beta_r \\ &= RC_1 . \end{aligned} \tag{25}$$

Here C_1 is a constant which depends on the probability density of b and β_r. By dealing with the probability that $R(t) < R$ in much the same way and then dividing by (25), we can show that the average length of the intervals during which $R(t) < R$ is

$$\bar{t} \approx RC_2 \tag{26}$$

where C_2 is a constant of the same nature as C_1 and R is again small.

Equation (25) says that, for a given experimental run, the average number of times per minute the signal drops below $R/2$ microvolts should be half the number of times it drops below R microvolts, R being very small. Furthermore, from (26), fades below $R/2$ microvolts should last, on the average, only half as long as the fades below R. These relations should hold for small values of R even though the experimentally observed ratios for the larger values of R may not agree with Table II.

The same sort of argument may be applied to the fade length distribution. As R becomes small, $F_r(u, R)$ approaches a definite function of $u = \tau/\bar{t}$, say $\varphi(u)$, provided u is not too large. Let R have the same significance as in (25). Then the probability that $R(t)$ will remain less than R for an interval lasting longer than τ seconds is approximately

$$\frac{R}{N_R}\int_0 \int_0^\infty b^{-1}\sqrt{\frac{\beta_r}{2\pi}}\,\varphi\left[\frac{2\tau}{R}\sqrt{\frac{\beta_r}{2\pi}}\right] g(b, \beta_r)\, db\, d\beta_r = \Phi(\tau/R), \quad (27)$$

where N_R is given by (25). Thus the probability depends on τ and R only through the ratio τ/R when R is small. The curves of Fig. 3 corresponding to the smaller values of R show this behavior (as indeed they should). For example, the curve for $R = 0.125$ is obtained almost exactly by shifting the curve for $R = 0.50$ to the left by an amount corresponding to quartering the fade lengths.

As an illustration of how the averaging process (27) may change $F_r(u, R)$, we suppose that the median level remains fixed at $R = 1.18$ while the rate of fluctuation changes in such a way as to formally carry the normal-law power spectrum (20) over into the power spectrum.

$$w(f) = \pi k^2\,[k^2 + 4\pi^2(f - f_0)^2]^{-3/2}.$$

This particular example is chosen so as to simplify the steps which follow. Instead of introducing $g(b, \beta_r)$ and averaging over β_r it is more convenient to average over the σ of (20). Some mathematical experimentation indicates that we should take

$$(k^2/4\pi^2\sigma^3)\exp\,[-k^2/8\pi^2\sigma^2]d\sigma \quad (28)$$

to be the probability that σ lies in the small interval $d\sigma$ because this choice makes the integral from $\sigma = 0$ to $\sigma = \infty$ of the product of (28) and (20) give the required $w(f)$. When we give β_r the value $(2\pi\sigma)^2$ indicated by (21), the φ function in (27) becomes

$$\varphi\left[\frac{\tau\sigma 2\sqrt{2\pi}}{R}\right] \quad (29)$$

where we take $\varphi(u)$ to be the limiting form of $F_r(u, R \to 0)$ given by (23). The integral (25) now gives $N_R = Rk/2$ and the integral in (27) becomes the integral from $\sigma = 0$ to $\sigma = \infty$ of the product of (28) and (29). The integration can be performed and gives

$$\Phi(\tau/R) = \left[1 + \frac{u^2}{4}\right]^{-1/2}\left[1 + \frac{u^2}{2} + u\sqrt{1 + \frac{u^2}{4}}\right]^{-1}, \quad (30)$$

where $u = k\tau/R$. This is the fade length distribution, when R is small,

which results when the median level remains fixed but the rate of fading fluctuates according to the law (28). The average value $\bar{t}$ of the fade length works out to be R/k, so that $u = \tau/\bar{t}$ in (30), in agreement with our earlier notation.

If we were to take σ^ν in place of σ^3 in (28) (and change the multiplying constant) we could obtain a more general, but also more complicated, expression for $\Phi(\tau/R)$. When $\nu = 2$ the power spectrum (24) is obtained but the integrals (25) and (27) corresponding to N_R and $\Phi(\tau/R)$ do not converge.

The expression (30) is plotted as a function of u in Fig. 4, along with $F_r(u, R \rightarrow \infty)$ and $F_r(u, R \rightarrow 0)$, given respectively by (22) and (23), for comparison. As u increases, (30) ultimately decreases as $2/u^3$. It is seen that the $\Phi(\tau/R)$ given by (30) and $F_r(u, R \rightarrow 0)$ [from which (30) is derived] are quite different in appearance for small values of u. The distribution for fixed median and fixed fading rate is $F_r(u, R \rightarrow 0)$, while the $\Phi(\tau/R)$ of (30) corresponds to a fixed median but a variable fading rate. It appears from (27) that many different $\Phi(\tau/R)$'s [of which (30) is only one] may be obtained by averaging over the median values and fading rates with different weighting functions $g(b, \beta_r)$. At this stage we are unable to tell from either theory or experiment whether a different $\Phi(\tau/R)$ will be required for each set of data, or whether there are only two or three universal types of $\Phi(\tau/R)$'s which will fit, for small R, all kinds of fading data.

Suppose that we are given a set of experimental results on short-term fading. How can we go about analyzing them to see whether they have anything in common with our theory?

One of the easiest things to test is how N_R, the average number of fades per second below the level R, depends on R. According to (25), N_R should be proportional to R when R is small, and, if the short-term median value and the rate of fading have remained fixed throughout the experiment, the ratios of N_R/N_1 should agree with those of Table II. From (26) the same is true of $\bar{t}$ and $\bar{t}/\bar{t}_1$. However, when the short-term median value and the rate of fading fluctuate, N_R and $\bar{t}$ should still be proportional to R when R is small, but the ratios in Table II may no longer hold. It should be noted that Table II lists values of both N_R/N_1 and $\bar{t}/\bar{t}_1$, and it may turn out that one set of ratios will agree better with experiment than the other. This may happen because N_R and $\bar{t}$ do not depend on b and β_r in the same way. N_R depends on both β_r and b, $\bar{t}$ only on β_r, and the probability that $R(t) < R$ (which, for small R, becomes $R^2/2b$) depends only on b. In fact, the deviations from Table II and from the Rayleigh distribution should give clues to the variation of b and β_r.

When experimental fade-length distributions for several levels of R are available, it is instructive to plot them on semi-log paper as a function of τ/R in much the same way as $F_r(u, R)$ is plotted as a function of u in Fig. 2. As R becomes small the curves should tend to coincide, at least when τ/R is not too large. This follows from (27). If the limiting curve can be made to coincide with the $R = 0$ curve in Fig. 2 by changing the scale of τ/R, then it is likely that the other curves in Fig. 2 and the curves of Fig. 3 will be valid. This indicates that b and β_r did not change much during the experiment.

If, on the other hand, the limiting curve looks like those of Fig. 13 or like the $\Phi(\tau/R)$ of Fig. 4, the probability of long fades is much greater. In this case one should plot on semi-log paper R times the probability that the fade length exceeds τ versus τ/R^2. For large τ and small R, the points should tend to lie on a common curve, which becomes a straight line as τ/T^2 becomes large. This behavior is suggested by one of the conjectures of Appendix IV concerning long fades when $w(f)$ behaves like (24) near f_0, k being very small (i.e., much power in the frequencies corresponding to slow fluctuations). It is assumed that $w(f)$ is still such that $\bar{t}$ exists. For $w(f)$'s of this sort the conjecture says that when τ is very large and R is small

$$P(\tau, R) = F_r(u, R) \to 4\bar{t}kR^{-2} \sum_{i=1}^{\infty} e^{-\alpha_i k\tau} \tag{31}$$

where $P(\tau, R)$ is the probability that a fade below level R will last longer than τ seconds. In (31) the median value of $R(t)$ is 1.18 and α_i is $j_i^2 R^{-2}$, j_i being the ith zero of $J_0(x)$.

From (11), $\bar{t}$ is proportional to R and it follows that $RP(\tau, R)$ tends to be a function of τ/R^2. This is the basis for the method of plotting described above. When τ is very large, only the first term in (31) is important, and it gives a straight line on the semi-log paper. As R increases, α_1 is no longer given by $5.78\, R^{-2}$. For $R = 1$, $\alpha_1 \approx 5.0$ and for $R =$ median $= 1.18$, $\alpha_1 \approx 3.25$.

Unfortunately we do not have any clear-cut rules to tell when, as τ increases, the fade-length distribution changes from a function of τ/R to $1/R$ times a function of τ/R^2.

Sometimes experimental results are given in the form of curves showing the average number of fades per hour, say $H(\tau, R)$, below the level R which last longer than τ seconds. According to (25) and (27), $H(\tau, R)$ should take the form $3600\, N_R\Phi(\tau/R) = \mathrm{C}R\Phi(\tau/R)$, where C is a constant, R is small, and τ/R not too large. Under the conditions leading to (31), we expect $H(\tau, R)$ to be of the form $\Psi(\tau/R^2)$ when τ is large and R is small. In fact, if we assume (31) and note that $N_R\bar{t}$ approaches

$R^2/2$ [b is one in (31), so that the median value here is 1.18],

$$H(\tau, R) \to 7200\, k \exp[-5.78\, k\tau/R^2]. \tag{32}$$

Since this expression contains only oue parameter, k, and is based on a number of assumptions, it is probably too simple to agree well with experiment. Nevertbeless, if the experimental data for $H(\tau, R)$ passes the test of being of the form $\Psi(\tau/R^2)$ for large τ and small R, it would be interesting to go one step farther and see how well the data can be fitted by a suitable choice of k in (32).

It is interesting to examine Fig. 13 of Ref. 1 in the light of the above results. This figure, with some dashed lines added, is reproduced here as Fig. 5. The three solid lines give the observed (for 505 mc) number of fades per hour which were more than 5, 10 and 15 db below the hourly median level and lasted longer than the time intervals shown on the abscissa scale. The two dashed straight lines labeled (a) show the 5- and 15-db curves obtained by applying our results to the 10-db curve in the following way. The number of fades per hour of depth R of duration longer than τ seconds is $H(\tau, R)$ which, when R is small and τ/R not too large, may be written as

$$H(\tau, R) = CR\Phi(\tau/R), \tag{33}$$

where C is a constant. The values of R corresponding to the 5-, 10-, 15-db curves are in the ratio of 1.78, 1, 0.56. Since the curves of Fig. 5 are plots of $H(\tau, R)$ versus τ, (33) gives a relation between them. Thus, suppose the coordinates (τ_1, H_1) of a point on the R_1 curve are known. Then the coordinates of the point (τ_2, H_2) corresponding to the same value of τ/R on the R_2 curve are given by

$$\begin{aligned} \tau_2 &= \tau_1 R_2/R_1, \\ H_2 &= H_1 R_2/R_1. \end{aligned} \tag{34}$$

The 15-db dashed line (a) was obtained by taking the solid 10-db line to be the R_1 curve and using (34) with $R_2/R_1 = 0.56$. The 5-db dashed line (a) was obtained in a similar way from the 10-db line by taking $R_2/R_1 = 1.78$, even though this may take us into the regiou where our approximation begins to fail. The dasbed lines (a) are drawn only for the smaller values of τ/R because of our assumption that (33) may not hold if τ/R is too large.

Under certain conditions we may expect $H(\tau, R)$ to depend only on the ratio τ/R^2 when τ is large and R is small. The dashed straight lines labeled (b) are obtained from the 10-db curve by assuming $H(\tau, R)$ to

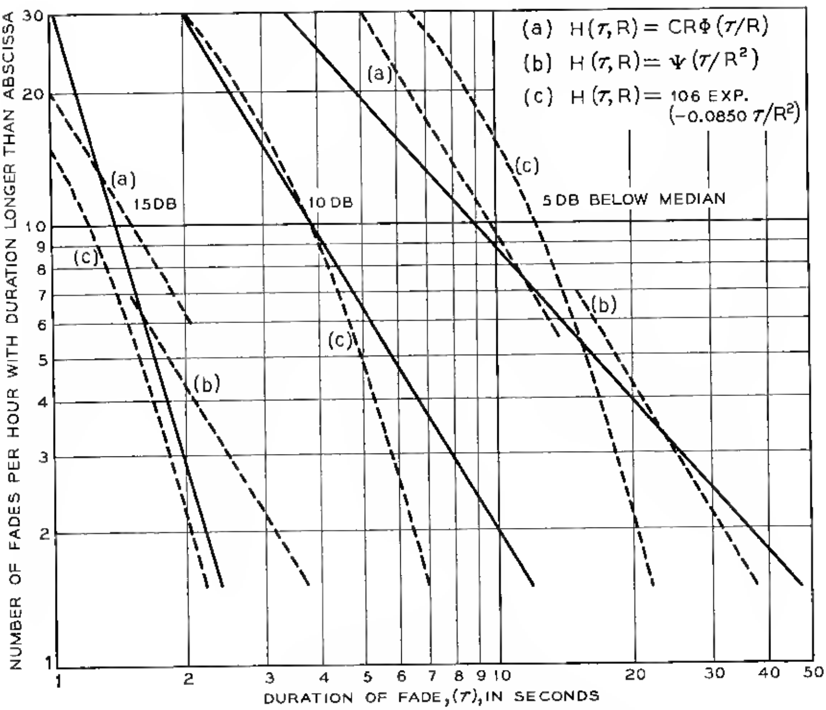

Fig. 5 — Number vs. duration of fast fades at 505 mc.

be of the form $\psi(\tau/R^2)$ and proceeding in much the same way as in the calculation of the lines (a). The lines (b) are drawn only for the larger values of τ/R^2 because τ is supposed to be large.

The curved dashed lines labeled (c) in Fig. 5 are plots of $H(\tau, R)$ computed from (32), with k chosen so that $H(\tau, R)$ agrees with the experimental 10-db result at the ordinate corresponding to ten fades per hour. Since the value of R, 10 db below the median value of 1.18, is 0.372, and since $\tau = 3.8$ seconds corresponds to ten fades per hour, the equation to determine k is

$$H(3.8, 0.372) = 10. \tag{35}$$

This yields two values of k, namely 0.0018 and 0.0147. The value 0.0147 was used in plotting the curves (c) in Fig. 5, since the other value gives curves with much smaller slopes.

The difference between the dashed curves in Fig. 5 and the corresponding solid curves is noticeable. An examination of the original data indi-

cates that some of the discrepancy may be due to the fact that, in one of the experimental runs, N_R for 10 db exceeds the N_R for 5 db. This completely contradicts (25) and is probably caused by the short-term median (as measured by the parameter b) temporarily dropping down to a low value. This violates our assumption of R being "small". The relation between the 10-db and 15-db experimental results seems to agree fairly well with the theory, but comparison is difficult because of the scantiness of the 15-db data.

Our results for $R(t)$ may also be compared with some experimental results given by R. R. Favreau, H. Low and I. Pfeffer.[6] Their work is concerned with the probability that in an interval of T seconds duration there will be at least one fade of depth R which lasts longer than τ seconds. They express this probability as $1 - \exp[-P'(0)f_bT]$, where f_b is the associated bandwidth, and their $P'(0)f_b$ may be roughly equated to our $N_RF_\tau(\tau/\bar{t}, R)$. Although the comparison is not straightforward, it appears that there is fairly good agreement for values of R larger than 0.25. As R decreases below 0.25 a disturbing discrepancy between experiment and theory seems to creep in. The reasons for this are not clear.

Although in this paper we are primarily concerned with rapid fading and have been speaking about it in this section up until now, it is of some interest to try to apply our theory to the slow fades, i.e., to the distribution of the hourly medians. Since the hourly medians have a distribution which is nearly normal in decibels, it is natural to compare the observed statistics with those of a Gaussian noise current $I(t)$. In this comparison "db above the median" plays the same role as "amperes".

When the fade-length distributions given in Figs. 6 and 7 of Ref. 1 are plotted on semi-log paper the resulting points tend to lie on straight lines instead of on curves shaped like those of Fig. 1. This exponential distribution of fade lengths indicates that the power spectrum of $I(t)$ is more like the ones discussed in Section IX and Appendix IV than like the normal type shown in equation (16). A stochastic process which does have an exponential distribution of fade lengths may be constructed by drawing a value at random from a normal universe every hour on the hour. However, the successive values in such a process would be uncorrelated. This is not true for the hourly medians.

Even though we have little justification for doing so, it is interesting to compare the separation between the experimental curves for various depths of fades with the separation predicted by the analogue of equa-

tion (27). The analogue states that the probability of $I(t)$ remaining less than $-I$ for an interval lasting longer than τ is approximately of the form $\Phi(\tau I)$ when I is large. According to this rule, the -10-db curves in Figs. 6 and 7 of Ref. 1 may be obtained by shifting the -5-db curves to the left by an amount corresponding to changing the time scale in the ratio 5 to 10 (or 1 to 2). Actually, a ratio of 1 to 3 would be required to agree with the experimental results. The analogue of (31) suggests in a vague way that when τ becomes large, I remaining large, the function $\Phi(\tau I)$ might change into a function of τI^2. This would correspond to changing the time scale in the ratio of 1 to 4. However, not much significance can be attached to these figures.

V. DISTRIBUTION OF THE LENGTHS OF THE INTERVALS DURING WHICH $I(t) > I$

In Section II we have given expressions for the average length $\bar{l}$ and the expected number per second N_I of the intervals during which $I(t)$ exceeds the value I. As a first step in finding the probability $p(\tau, I)\, d\tau$ that the length of such an interval lies between τ and $\tau + d\tau$, we obtain an approximation, $p_1(\tau, I)\, d\tau$, which agrees well with $p(\tau, I)\, d\tau$ for small values of τ. The expression $p_1(\tau, I)\, d\tau$ is the probability that, if $I(t)$ passes upward through the value I at time t_1, it will pass downward through I in the infinitesimal interval t_2, $t_2 + d\tau$ where $t_2 = t_1 + \tau$.

An expression for $p_1(\tau, I)$ may be obtained by the method outlined in Section 3.4 of Ref. 2. Thus, the probability that $I(t)$ will pass upwards through the level I in t_1, $t_1 + dt_1$ and downwards through I in t_2, $t_2 + dt_2$ is

$$- dt_1\, dt_2 \int_0^\infty dI_1' \int_{-\infty}^0 dI_2' I_1' I_2' p(I, I_1', I_2', I), \tag{36}$$

where $p(I_1, I_1', I_2', I_2)$ denotes the probability density of $I(t_1)$, and $I'(t_1)$, $I'(t_2)$, $I(t_2)$ and the primes denote time derivatives. Then

$$p_1(\tau, I)\, dt_2 = \frac{\text{expression (36)}}{\text{prob of } I(t) \text{ passing upward through } I \text{ in } t_1,\, t_1 + dt_1} \tag{37}$$

and we obtain

$$p_1(\tau, I) = -2\pi\beta^{-1/2} e^{I^2/2} \int_0^\infty dI_1' \int_{-\infty}^0 dI_2' I_1' I_2' p(I, I_1', I_2', I). \tag{38}$$

Here β is given by equation (4) and we have taken $b = \overline{I^2(t)} = 1$.

The probability density $p(I_1, I_1', I_2', I_2)$ is

$$(2\pi)^{-2}M^{-1/2} \exp\left\{-\frac{1}{2M}[M_{11}I_1^2 + 2M_{12}I_1I_1' + 2M_{13}I_1I_2' \right.$$
$$+ 2M_{14}I_1I_2 + M_{22}I_1'^2 + 2M_{23}I_1'I_2' \tag{39}$$
$$\left. + 2M_{24}I_1'I_2 + M_{33}I_2'^2 + 2M_{34}I_2'I_2 + M_{44}I_2^2]\right\},$$

where M_{ij} is the cofactor of the ijth element in the determinant

$$M = \begin{vmatrix} 1 & 0 & m' & m \\ 0 & \beta & -m'' & -m' \\ m' & -m'' & \beta & 0 \\ m & -m' & 0 & 1 \end{vmatrix} \tag{40}$$

in which we have simplified the notation of Ref. 2 by writing

$$m = \psi_\tau = \int_0^\infty w(f) \cos 2\pi f\tau \, df,$$
$$m' = dm/d\tau, \qquad m'' = d^2m/d\tau^2, \qquad \beta = [-m'']_{\tau=0}. \tag{41}$$

The values of the M_{ij}'s and some relations among them are listed in Appendix I. When I_1 and I_2 are set equal to I and use is made of the fact that some of the M_{ij}'s are equal, the exponent in (39) reduces to $-1/(2M)$ times

$$2(M_{11} + M_{14})I^2 + 2(M_{12} + M_{24})(II_1' - II_2') + M_{22}(I_1'^2 + I_2'^2)$$
$$+ 2M_{23}I_1'I_2'. \tag{42}$$

Replacing I_1', I_2' in (42) by $x_1 - a_1$, $x_2 - a_2$, choosing the a's so as to make the first order terms in x_1 and x_2 vanish and using

$$(M_{12} + M_{24})(1 + m) = m'(M_{22} - M_{23})$$
$$M = (M_{11} + M_{14})(1 + m) - m'(M_{12} + M_{24}) \tag{43}$$

gives

$$a_1 = -a_2 = m'I/(1 + m) \tag{44}$$

and converts (42) into

$$M_{22}(x_1^2 + x_2^2) + 2M_{23}x_1x_2 + 2I^2M(1 + m)^{-1}. \tag{45}$$

When the change of variable corresponding to

$$\begin{aligned} x(1 - r^2)^{-1/2} &= x_1(M_{22}/M)^{1/2} \\ y(1 - r^2)^{-1/2} &= -x_2(M_{22}/M)^{1/2} \\ r = M_{23}/M_{22} &= \frac{m''(1 - m^2) + mm'^2}{\beta(1 - m^2) - m'^2} \end{aligned} \tag{46}$$

is made in (38) it goes into

$$p_1(\tau, I) = M_{22}\beta^{-1/2}(1 - m^2)^{-3/2} \exp\left[\frac{I^2}{2} - \frac{I^2}{1 + m}\right] J(r,h), \tag{47}$$

where

$$\begin{aligned} J(r, h) &= \frac{1}{2\pi s} \int_h^\infty dx \int_h^\infty dy (x - h)(y - h)e^z, \\ h &= \frac{m'I}{1 + m}\left[\frac{1 - m^2}{M_{22}}\right]^{1/2}, \qquad s = (1 - r^2)^{1/2}, \end{aligned} \tag{48}$$

$$\begin{aligned} M_{22} &= \beta(1 - m^2) - m'^2, \\ z &= -\frac{x^2 + y^2 - 2rxy}{2(1 - r^2)} = -2^{-1}s^{-2}(x^2 + y^2 - 2rxy), \end{aligned} \tag{49}$$

and we have used

$$(1 - m^2)M = M_{22}^2 - M_{23}^2 = M_{22}^2(1 - r^2). \tag{50}$$

$J(r, h)$ may be expressed in terms of the tabulated double integral

$$K(r, h) = \frac{1}{2\pi s} \int_h^\infty dx \int_h^\infty dy\, e^z \tag{51}$$

as follows. We have

$$\frac{\partial}{\partial x} e^z = s^{-2}(ry - x)e^z,$$

$$\frac{\partial}{\partial y} e^z = s^{-2}(rx - y)e^z.$$

Elimination of the y terms on the right leads to

$$\left(\frac{\partial}{\partial x} + r\frac{\partial}{\partial y}\right) e^z = -xe^z. \tag{52}$$

In much the same way, elimination of the x^2 and y^2 from the second partial derivatives gives

$$\left[r\frac{\partial^2}{\partial x^2} + r\frac{\partial^2}{\partial y^2} + (1 + r^2)\frac{\partial^2}{\partial x \partial y}\right] e^z = xye^z - re^z. \tag{53}$$

When the integrand in $J(r, h)$ is written as $(xy - hx - hy + h^2)e^z$ and use is made of (52), (53) and the symmetry in x and y, we obtain

$$\begin{aligned} J(r, h) &= \frac{1}{2\pi s}\int_h^\infty dx \int_h^\infty dy \left[2r\frac{\partial^2}{\partial y^2} + (1 + r^2)\frac{\partial^2}{\partial x \partial y}\right. \\ &\qquad \left. + r + 2h(1 + r)\frac{\partial}{\partial y} + h^2\right] e^z \\ &= (r + h^2)K(r, h) + (s/2\pi)\exp\left[-\frac{h^2}{1 + r}\right] - h(2\pi)^{-1/2}e^{-h^2/2}[1 - P(a)] \end{aligned} \tag{54}$$

where $P(a)$ is the error integral defined by (3) and

$$a = h\left[\frac{1 - r}{1 + r}\right]^{1/2}, \qquad \frac{h^2}{1 + r} = \frac{a^2 + h^2}{2}. \tag{55}$$

Values of $K(r, h)$ may be obtained from tables[8] of d/N. This is true because d/N is the function of the three variables r, h, k obtained from the right-hand side of (51) by changing the lower limit of integration in the y integral from h to k. The tables do not extend to negative values of h, and $K(r, h)$ for these values must be obtained from

$$K(r, -h) = K(r, h) + P(h). \tag{56}$$

From (56) it may be shown that

$$\begin{aligned} p_1(\tau, -I) = p_1(\tau, I) + \frac{M_{22}}{\beta^{1/2}(1 - m^2)^{3/2}} &\left[(r + h^2)P(h) + \frac{2he^{-h^2/2}}{\sqrt{2\pi}}\right] \\ &\exp\left[\frac{I^2}{2} - \frac{I^2}{1 + m}\right] \end{aligned} \tag{57}$$

where h depends on I in accordance with (48).

The following special values of $K(r, h)$ and $J(r, h)$ may be derived directly from known results.

1. When $h = 0$

$$\begin{aligned} K(r, 0) &= \frac{1}{2} - \frac{\cos^{-1} r}{2\pi}, \qquad 0 < \cos^{-1} r \leq \pi \\ J(r, 0) &= rK(r, 0) + \frac{s}{2\pi}. \end{aligned} \tag{58}$$

2. When $r = 0$

$$\begin{aligned} s &= 1, \qquad a = h, \\ K(0, h) &= \tfrac{1}{4}[1 - P(h)]^2, \\ J(0, h) &= \left\{\frac{h}{2}[1 - P(h)] - (2\pi)^{-1/2}e^{-h^2/2}\right\}^2. \end{aligned} \tag{59}$$

3. When r approaches unity from below we have, in the limit,

$$\begin{aligned} s &= 0, \qquad a = 0, \\ K(1, h) &= \tfrac{1}{2}[1 - P(h)], \\ J(1, h) &= 2^{-1}(1 + h^2)[1 - P(h)] - h(2\pi)^{-1/2}e^{-h^2/2}. \end{aligned} \tag{60}$$

4. When h approaches $-\infty$, $K(r, \infty)$ approaches one and $J(r, h)$ is approximately $h^2 + r$.

As τ becomes very large $p_1(\tau, I)$ approaches the value of N_I which is

$$(2\pi)^{-1}\beta^{1/2} \exp(-I^2/2). \tag{61}$$

This follows from considerations of the type which led to (5). It may also be derived from (47), (48) and the fact that m, m', m'' all approach zero as τ becomes large. In this case M_{22} approaches β, and r and h become zero.

When I is zero, equation (47) reduces to a result given in Ref. 2, namely

$$p_1(\tau, 0) = M_{22}\beta^{-1/2}(1 - m^2)^{-3/2}[r(\pi - \cos^{-1} r) + s]/2\pi, \tag{62}$$

where $0 < \cos^{-1} r < \pi$.

Expressions for the various parameters entering the expression for $p_1(\tau, I)$ when τ is small are given in Appendix II. Combining the results of Appendix II with (47), we obtain

$$\begin{aligned} p_1(\tau, I) &\approx (\tau B/4\beta) \exp(-I^2\tau^2\beta/8)J(1, h) \\ h &\approx -I\beta B^{-1/2} \end{aligned} \tag{63}$$

where τ is assumed to be small and B is given by one of equations (125). There are two cases to be considered. In the first one, I remains fixed as τ approaches zero. It then follows that $p_1(\tau, I)$ approaches zero linearly with τ according to

$$p_1(\tau, I) \approx (\tau B/4\beta)J(1, h) \tag{64}$$

where $J(1, h)$ and h are given by (60) and (63). In the second case, I is positive and increases as τ decreases so as to keep the order of τI at

unity. Tben h approaches $-\infty$ and $J(1, h)$ is approximately h^2, with the result that

$$p_1(\tau, I) \approx (\beta\tau I^2/4) \exp(-I^2\tau^2\beta/8). \tag{65}$$

This expression may also be obtained from (47) by first letting I become large (assuming m' to be negative so that h becomes large and negative) and then letting τ become small.

When the right-hand side of (65) is integrated from $\tau = 0$ to $\tau = \infty$ the result is unity. Since the same is true of the exact probability density $p(\tau, I)$ [to which $p_1(\tau, I)$ is a first approximation], and since $p_1(\tau, I) \geqq p(\tau, I)$, we are led to expect that

$$p(\tau, I) \to (\beta\tau I^2/4) \exp(-I^2\tau^2\beta/8) \tag{66}$$

when I becomes large and positive (and τI remains fixed). A formal proof of (66) has been constructed on the assumptions (i) that $p(\tau, I)$ ultimately decreases exponentially as τ becomes large, and (ii) that m' remains negative for all positive values of τ. The second assumption seems to be required by the method of proof rather than by nature. We shall not give the proof here because of its length. Instead, we shall outline a method by which (66) may be obtained directly.* This method is due to D. S. Palmer and grew out of correspondence with him.

When I is very large, the intervals during which $I(t) > I$ are very short. The length of an interval starting at $t = t_1$ is, to a second degree Taylor approximation,

$$l = 2I'(t_1)/[-I''(t_1)].$$

The joint probability density of $I(t)$ and its first two derivatives is

$$(2\pi)^{-3/2}(\beta B)^{-1/2} \exp\left[-\frac{I^2}{2} - \frac{I'^2}{2\beta} - \frac{(I'' + \beta I)^2}{2B}\right]$$

where B is given by (125). Since I'' is a random variable whose mean value $-\beta I$ is large compared to its standard deviation, we may put $l = 2I'(t_1)/\beta I$.

The chance that $I(t)$ will pass upwards through the value I in the interval t_1, $t_1 + dt$ with a slope between I' and $I' + dI'$ is equal to the chance that, at time t_1, $I(t)$ lies between I and $I - I'dt$ and bas a slope in I', $I' + dI'$. This chance is

$$\frac{(I'\,dt)(dI')}{2\pi\sqrt{\beta}} \exp\left[-\frac{I^2}{2} - \frac{I'^2}{2\beta}\right].$$

* Another proof has subsequently been devised by Mark Kac and D. Slepian. Also see the end of Appendix III.

Expressing I' in terms of l shows that the chance of $I(t)$ passing up through I in t_1, $t_1 + dt$ and starting an $I(t) > I$ interval whose length lies between l and $l + dl$ is

$$[\beta^{3/2} I^2 l \, dl \, dt/8\pi] \exp \left[-\frac{I^2}{2} - \frac{\beta I^2 l^2}{8} \right]. \tag{67}$$

Our goal of obtaining the probability density (65) for the lengths of the $I(t) > I$ intervals, I very large, is now within reach. All that remains to be done is to divide (67) by the chance $[\beta^{1/2} dt/2\pi] \exp [-I^2/2]$ that $I(t)$ will pass upwards across I in t_1, $t_1 + dt$.

In much of the following work it is convenient to use the variable u, defined by

$$u = \tau/\bar{t}, \qquad \bar{t} = \pi\beta^{-1/2}[1 - P(I)] \exp (I^2/2), \tag{68}$$

where the expression for the average duration $\bar{t}$ is obtained by setting $b = 1$ in (6). The probability density $f(u, I)$ of u is related to the probability density $p(\tau, I)$ of τ by

$$f(u, I) = \bar{t} p(u\bar{t}, I), \tag{69}$$

and the cumulative probability

$$F(u, I) = \int_u^\infty f(u, I) \, du \tag{70}$$

has already appeared, for the special $w(f)$ given by (16), in Section III. The first approximation to $f(u, I)$ corresponding to $p_1(\tau, I)$ is

$$f_1(u, I) = \bar{t} p_1(u\bar{t}, I). \tag{71}$$

When u becomes very large $f_1(u, I)$ approaches the value $[1 - P(I)]/2$.

The function $f(u, I)$ has the following limiting forms:

$$\begin{aligned} f(u, I) &\to (u\bar{t}^2 B/4\beta) J(1, h), && u \to 0 \\ f(u, I) &\to (\pi u/2) \exp (-u^2\pi/4), && I \to \infty \\ f(u, I) &\to \exp (-u), && I \to -\infty, u > 0. \end{aligned} \tag{72}$$

The first of these follows from (64), the second from (66) and the second of equations (6) and the third expresses the exponential behavior which sets in after $f(u, I)$ has passed through its maximum value (which occurs close to $u = 0$ when I is large and negative). The exponential law is followed because most of the intervals are so long that the probability of an interval of length τ ending in τ, $\tau + d\tau$ is independent of τ.

VI. APPROXIMATIONS FOR LONG INTERVALS

It is generally assumed that, for large values of τ, $p(\tau, T)$ decreases exponentially. This assumption is supported by the following informal argument, which is much the same as the one used at the end of Section V for the case $I = -\infty$. When $I(t)$ remains greater than I for an interval long in comparison with the effective range of the autocorrelation, $I(t)$ "forgets" when it entered the region $I(t) > I$. After this amnesia occurs it wanders about in the region in a fashion independent of its entrance time, until it happens to drop below the value I and thus end the interval. The exponential decrease is obtained when it is assumed that the chance of dropping below the value I in the interval t, $t + \Delta t$ depends only on Δt and not on how long $I(t)$ has been in the region.

However, no one seems to have given an exact and usable asymptotic formula for this exponential decrease, although progress in this direction has been made by Kuznetsov, Stratonovich and Tikhonov.[9] When applied to our problem, their result gives $F(u, I)$ as an exponential function of an infinite series whose nth term is a multiple integral of order $n - 1$. When τ becomes large each term approaches the form $a_n\tau + b_n$, where a_n and b_n are independent of τ. Here we shall be content to connect, by eye, the curve showing our estimates of $p(\tau, I)$ for small values of τ (obtained from $p_1(\tau, I)$) with an exponential curve chosen so as to (i) make the area under $p(\tau, I)$ unity and (ii) give the correct average value for τ. It is hoped that this will give an estimate of some use in engineering applications, even though it may not contribute a great deal to our understanding of the behavior of $p(\tau, I)$ for very large values of τ.

We shall work with $u = \tau/\bar{t}$, its probability density $f(u, I)$ defined by (69), and the approximation $f_1(u, I)$ defined by (71). The procedure consists of calculating

$$F_1(u, I) = 1 - \int_0^u f_1(v, I)\, dv \tag{73}$$

$$G_1(u, I) = 1 - \int_0^u F_1(v, I)\, dv \tag{74}$$

by numerical integration and plotting F_1 versus G_1 as shown by the solid line in Fig. 6. The curve starts at the point (1, 1), corresponding to $u = 0$, and curves in towards the origin as u increases, eventually crossing the G axis as shown. With the (G_1, F_1) curve as a guide, we draw in the (G, F) curve shown by the dashes. This curve is drawn so as to coincide with the solid curve in the region around (1, 1) and then depart from it in a "reasonable" manner so as to pass through the origin. Once the (G, F) curve is determined, the relation between G and u may be

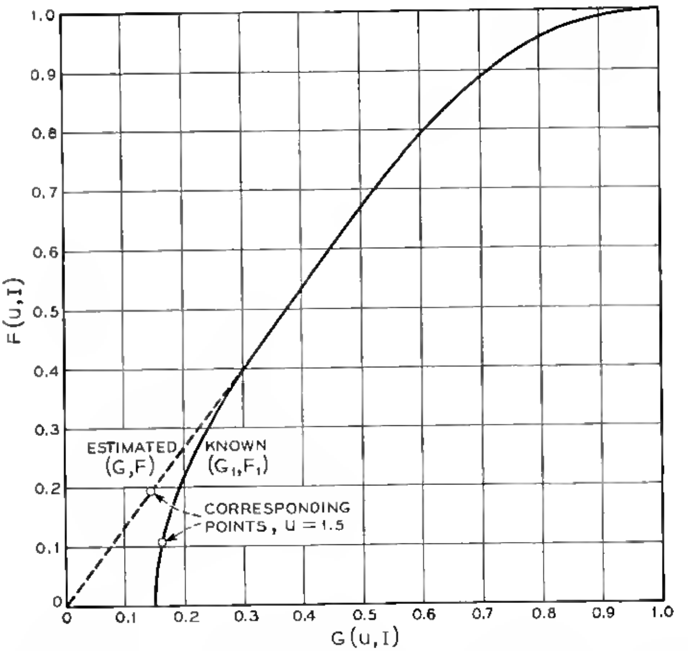

Fig. 6 — Method used to estimate probability distribution $F(u, I)$ for large values of u. These curves are for $I = 0$ and the normal-law power spectrum (16).

determined by numerical integration from

$$u = \int_G^1 \frac{dG}{F(G)} \tag{75}$$

and from this the cumulative probability $F(u, I)$ may be obtained as a function of u.

The justification of this procedure follows from the fact that functions $F(u, I)$, $G(u, I)$, computed from $f(u, I)$ (assumed known for the moment) by omitting the subscripts in (73) and (74), define a curve on Fig. 6 which starts at (1, 1) for $u = 0$ and reaches the origin at $u = \infty$. Thus

$$\begin{aligned} F(\infty, I) &= 1 - \int_0^\infty f(v, I)\, dv = 0, \\ G(\infty, I) &= 1 - \int_0^\infty F(v, I)\, dv \\ &= 1 - \int_0^\infty vf(v, I)\, dv = 0, \end{aligned} \tag{76}$$

$$p_2(\tau, 0) = \frac{N^2}{4\pi(\beta N_{66})^{1/2} N_{22} N_{33} D_3} \left[\frac{1 + a - b - c}{1 + a} - \frac{a - bc}{D_3^{1/2}} (\alpha_1 + \alpha_2 + \alpha_3 - \pi)\right] \tag{83}$$

where N_{ij} is the cofactor of the element ij in the determinant

$$N = \begin{vmatrix} 1 & 0 & m' & m & n \\ 0 & \beta & -m'' & -m' & -n' \\ m' & -m'' & \beta & 0 & n' \\ m & -m' & 0 & 1 & n \\ n & -n' & n' & n & 1 \end{vmatrix}$$

with n and n' being the values of m and m' computed for $\tau/2$. The other parameters are

$$a = -N_{23}(N_{22}N_{33})^{-1/2}, \qquad b = -N_{35}(N_{33}N_{55})^{-1/2},$$
$$c = N_{25}(N_{22}N_{55})^{-1/2},$$

$$\alpha_1 = \cot^{-1} \frac{a - bc}{D_3^{1/2}}, \qquad D_3 = \begin{vmatrix} 1 & c & b \\ c & 1 & a \\ b & a & 1 \end{vmatrix},$$

where $0 < \alpha_1 < \pi$ and α_2 and α_3 are obtained from α_1 by a cyclic permutation of a, b, c. It turns out that $b = c$ and $\alpha_2 = \alpha_3$. From the determinant N it may be shown that

$$\begin{aligned} N_{22} &= N_{33} = \beta A + B - m'^2(1 - n^2), \\ N_{23} &= m''A + B - m'^2(n^2 - m), \\ N_{25} &= -N_{35} = [n'(1 + m) - nm']C, \\ N_{55} &= [(\beta + m'')(1 + m) - m'^2]C, \\ N &= (N_{22}^2 - N_{23}^2)/A, \end{aligned}$$

where

$$A = (1 - m)(1 + m - 2n^2), \qquad B = n'(1 - m)[2m'n - n'(1 + m)],$$
$$C = (\beta - m'')(1 - m) - m'^2.$$

The second item is concerned with the approximate integral equation

$$p_1(\tau, I) = p(\tau, I) + \int_0^\tau p(y, I) q_1(\tau - y, I)\, dy \tag{84}$$

where $q_1(\tau, I)\, d\tau$ is the chance that $I(t)$ will pass downward through level I in $(\tau, \tau + d\tau)$, given that $I(t)$ passes downward through level I at $\tau = 0$. This is an extension of an equation given by D. S. Palmer.[5] When $I = 0$, (84) becomes McFadden's integral equation mentioned in the discussion following equation (19). Equation (84) is based on the assumption that the length of an $I(t) > I$ interval and the distance between the following downward crossings are independent. Changing the upper limit of integration for I_1' from ∞ to $-\infty$ on the right-hand side of (38) gives an expression for $q_1(\tau, I)$ which leads to

$$\begin{aligned} q_1(\tau, I) = p_1(\tau, I) + \left\{ M_{22}\beta^{-1/2}(1 - m^2)^{-3/2} \exp\left[\frac{I^2}{2} - \frac{I^2}{1+m}\right]\right\} \\ \left\{\frac{h}{\sqrt{2\pi}} \exp(-h^2/2) - \frac{(r + h^2)}{2}[1 - P(h)]\right\} \end{aligned} \tag{85}$$

in which the various parameters have the same meaning as in (47). When $I = 0$, the results (58) lead to

$$q_1(\tau, 0) = M_{22}\beta^{-1/2}(1 - m^2)^{-3/2}[s - r \cos^{-1} r]/2\pi.$$

VII. DISTRIBUTION OF INTERVAL LENGTHS FOR ENVELOPE

Here we study the envelope $R(t)$ of $I(t)$ in much the same way as $I(t)$ was studied in Section V. $I(t)$ is now taken to be a narrow-band Gaussian noise current whose power spectrum $w(f)$ is assumed to be symmetrical about the midband frequency f_0. We shall take $p(\tau, R)$ to be the probability density of the interval lengths during which $R(t)$ remains less than R. Strictly speaking, we should put some sort of a subscript, such as the r used on F in Section III, on $p(\tau, R)$ to distinguish it from the $p(\tau, I)$ of Section V. However, we shall not do so because the chance of confusion is small.

The first approximation to $p(\tau, R)$ is $p_1(\tau, R)$, where $p_1(\tau, R)\, d\tau$ is the chance that $R(t)$ will pass upwards through level R in $(t_2, t_2 + d\tau)$ given that $R(t)$ has passed downward through R at t_1, τ being the difference $t_2 - t_1$. Reasoning similar to that leading to (38) gives

$$\begin{aligned} p_1(\tau, R) = -\left(\frac{2\pi}{\beta}\right)^{1/2} R^{-1} e^{R^2/2} \int_{-\infty}^0 dR_1' \\ \int_0^\infty dR_2'\, R_1'\, R_2'\, p(R, R_1', R_2', R) \end{aligned} \tag{86}$$

where now $b = 1$ and β is the β_r of (8). The function $p(R_1, R_1', R_2', R_2)$ is the probability density of $R(t_1)$, $R'(t_1)$, $R'(t_2)$, $R(t_2)$ and the primes denote time derivatives.

Let $I_c(t)$ and $I_s(t)$ denote the "in-phase" and "quadrature" components associated with $R(t)$. Let I_{c1}, I_{c1}', I_{c2}', I_{c2} stand for the values of $I_c(t)$ and $I_c'(t)$ at t_1 and t_2, and similarly for $I_s(t)$. Because of the symmetry of $w(f)$ about f_0, the I_c's are independent of the I_s's and their joint distribution is

$$p(I_{c1}, I_{c1}', I_{c2}', I_{c2})p(I_{s1}, I_{s1}', I_{s2}', I_{s2}), \tag{87}$$

where these two functions may be obtained from (39) by adding the subscripts c and s, respectively, to the I_1's and I_2's. The β and m appearing in the expression (40) for M are now given by

$$\begin{aligned} m &= \int_0^\infty w(f)\cos 2\pi(f - f_0)\tau\, df, \\ \beta &= [-m'']_{\tau=0} \end{aligned} \tag{88}$$

instead of (41). These statements follow from results given in Appendix II of Ref. 3.

When we introduce the polar coordinates

$$\begin{aligned} I_{c1} &= R_1 \cos\theta_1 \qquad & I_{c2} &= R_2 \cos\theta_2 \\ I_{s1} &= R_1 \sin\theta_1 \qquad & I_{s2} &= R_2 \sin\theta_2 \end{aligned} \tag{89}$$

and their associated time derivatives, and then set

$$\begin{gathered} \varphi = \theta_1 - \theta_2, \qquad c = \cos\varphi, \qquad s = \sin\varphi, \\ R_1 = R_2 = R, \end{gathered} \tag{90}$$

the joint distribution (87) goes into

$$\begin{aligned} \frac{(2\pi)^{-4}}{M} \exp\Big\{ -\frac{1}{2M} [&(2M_{11} + cM_{14})R^2 + 2(M_{12} + cM_{24})(RR_1' - RR_2') \\ &+ M_{22}(R_1'^2 + R_2'^2) + 2cM_{23}R_1'R_2' \\ &+ M_{22}R^2(\theta_1'^2 + \theta_2'^2) + 2cM_{23}R^2\theta_1'\theta_2' \\ &+ 2sM_{23}R(R_1'\theta_2' - R_2'\theta_1') - 2sM_{24}R^2(\theta_2' + \theta_1')] \Big\}. \end{aligned} \tag{91}$$

The quantity $p(R,R_1',R_2',R)dR_1dR_2dR_1'dR_2'$ is obtained by multiplying (91) by

$$dI_{c1} \cdots dI_{s2} = R^4\, dR_1\, dR_2\, dR_1'\, dR_2'\, d\theta_1\, d\theta_2\, d\theta_1'\, d\theta_2'$$

and integrating θ_1, θ_2 from 0 to 2π, and θ_1', θ_2' from $-\infty$ to $+\infty$. One

of the integrations with respect to the θ's may be performed. We write the other as an integration with respect to φ. When the integrations with respect to θ_1' and θ_2' are performed $p(R, R_1', R_2', R)$ is found to be

$$\left(\frac{R}{2\pi}\right)^2 \int_0^{2\pi} (M_{22}^2 - c^2M_{23}^2)^{-1/2} e^A \, d\varphi \tag{92}$$

where A contains terms of the first and second degree in R_1', R_2'. Incidentally, the linear terms enter only in the combination $R_1' - R_2'$. Upon setting R_1', R_2' equal to $x_1 - a_1$, $x_2 - a_2$, respectively, and choosing a_1, a_2 so as to make the coefficients of x_1, x_2 in the resulting expression for A vanish we find

$$a_2 = -a_1, \tag{93}$$

$$(M_{22}^2 - M_{23}^2)a_1 = R\{M_{12}M_{22} + M_{23}M_{24} + c[M_{23}M_{12} + M_{22}M_{24}]\}.$$

The expressions given in (123) show that both sides of the equation for a_1 contain the factor M, which may be divided out with the result

$$a_1 = \frac{Rm'(c - m)}{1 - m^2}. \tag{94}$$

This choice of a_1 and a_2 and the results of Appendix I enable us to reduce (after a considerable amount of algebra) the expression for the exponent A in (92) to

$$-\frac{(1 - m^2)}{2(M_{22}^2 - c^2M_{23}^2)} [M_{22}(x_1^2 + x_2^2) + 2cM_{23}x_1x_2] - \frac{R^2(1 - mc)}{1 - m^2}. \tag{95}$$

When (92) is put in the expression (86) for $p_1(\tau, R)$ the result is a triple integral. The expression (95) suggests that we replace the variables R_1', R_2' by x, y defined by [see (46)]

$$x = -x_1[(1 - m^2)/M_{22}]^{1/2}, \qquad y = x_2[(1 - m^2)/M_{22}]^{1/2}, \qquad \rho = cM_{23}/M_{22}. \tag{96}$$

Then (86) goes into

$$p_1(\tau, R) = \frac{RM_{22}e^{R^2/2}}{(2\pi\beta)^{1/2}(1 - m^2)^2} \int_0^{2\pi} J(\rho, k) \exp\left[-\frac{R^2(1 - mc)}{1 - m^2}\right] d\varphi \tag{97}$$

where $J(\rho, k)$ is obtained from (48) by putting ρ, k for r, h and

$$\begin{aligned} k &= -a_1[(1 - m^2)/M_{22}]^{1/2} \\ &= \frac{Rm'(m - c)}{1 - m^2} \left(\frac{1 - m^2}{M_{22}}\right)^{1/2}, \end{aligned} \tag{98}$$

in which c stands for $\cos \varphi$. Here M_{22} and M_{23} are obtained by setting the values (88) for m and β in the appropriate expressions given in (120).

When τ becomes very large, k and ρ approach zero and we see that $p_1(\infty, R) = R(\beta/2\pi)^{1/2} \exp(-R^2/2)$ as it should according to (9). When τ approaches zero, with R fixed, the results of Appendix II enable us to show that

$$p_1(\tau, R) \to \frac{\tau R B}{2\beta\sqrt{2\pi}} \int_0^\infty J[1, R\beta B^{-1/2}(1 - x^2)] e^{-R^2x^2/2}\, dx$$

where $J(1, h)$ is given by (60).

The integral (97) must be evaluated numerically. However, a special case of interest in fading is obtained when R approaches zero. In this case, $p_1(\tau, R)$ tends to depend on τ and R only through the ratio τ/R. When we let τ and R both approach zero in such a way as to keep τ/R fixed, the results of Appendix II show that

$$\frac{M_{22}}{(1 - m^2)^2} \to \frac{B}{4\beta}, \qquad \frac{R^2(1 - mc)}{1 - m^2} \to \frac{R^2(1 - c)}{\beta\tau^2}, \qquad k \to -R(1 - c)2B^{-1/2}\tau^{-2}. \tag{99}$$

Therefore, k approaches $-\infty$ except when φ is zero, and $J(\rho, k)$ is approximately k^2 except in a negligibly small region around $\varphi = 0$. It is convenient to introduce the variable $u = \tau/\bar{l}$, which, in the present case, becomes, with the help of the approximation (11) for $\bar{l}$,

$$u \to \frac{2\tau}{R}\left(\frac{\beta}{2\pi}\right)^{1/2}. \tag{100}$$

The function of u corresponding to $p_1(\tau, R)$ is

$$f_1(u, R) = \bar{l} p_1(\tau, R), \tag{101}$$

and it follows from (99), (100) and (101) that as R approaches zero,

$$f_1(u, R) \to \frac{z^2}{2} \int_0^{2\pi} (1 - c)^2 \exp[-z(1 - c)]\, d\varphi, \qquad z = 2/(\pi u^2). \tag{102}$$

When we write $(1 - c)^2$ as $s^2 - 2c(1 - c)$ and integrate the s^2 portion by parts, we find that (102) may be expressed as a derivative:

$$\begin{aligned} f_1(u, R) &\to -\frac{d}{du} \frac{1}{\pi u} \int_0^{2\pi} c \exp[-2\pi^{-1}u^{-2}(1 - c)]\, d\varphi \\ &= -\frac{d}{du}\left[\frac{2}{u} I_1(z) e^{-z}\right] \end{aligned} \tag{103}$$

where $I_1(z)$ is a Bessel function of imaginary argument. It may be shown that the expression under the differentiation sign is unity when $u = 0$ and is zero when $u = \infty$. Hence, an argument similar to the one following equation (65) suggests that as R approaches zero the approximation $p_1(\tau, R)$ approaches the actual probability density $p(\tau, R)$. Then $f_1(u, R)$ approaches $f(u, R)$ and (103) is the limiting form of both. We also have

$$F(u, R) \to \frac{2}{u} I_1(2/\pi u^2) \exp(-2/\pi u^2) \tag{104}$$

where $F(u, R)$ is the probability that an interval during which $R(t) < R$ has a (normalized) length greater than u. $F(u, R)$ is the function denoted by $F_r(u, R)$ in Section III where equation (104) appears as equation (23). When u is very small or very large we have

$$\begin{aligned} &u \to 0, && u \to \infty, \\ &f(u, R) \to 3\pi u/8, && f(u, R) \to 6/\pi u^4, \\ &F(u, R) \to 1 - \tfrac{3}{16}\pi u^2, && F(u, R) \to 2/\pi u^3. \end{aligned} \tag{105}$$

The indefinite integral of the right-hand side of (104) is a constant plus

$$e^{-z}[I_0(z) + I_1(z)], \qquad z = 2/\pi u^2. \tag{106}$$

Equation (97) refers to the intervals for which $R(t) < R$. If we are interested in the intervals for which $R(t) > R$, the analogue $p_1^*(\tau, R)$ of $p_1(\tau, R)$ is obtained from (86) by changing the signs of the ∞'s in the limits of integration. Instead of $J(\rho, k)$ in the integrand of (97) we get a double integral similar to (48) except that the upper limits of integration are $-\infty$'s instead of ∞'s. This changes the $J(\rho, k)$ to $J(\rho, -k)$. Upon using (56), we obtain

$$\begin{aligned} p_1^*(\tau, R) &= p_1(\tau, R) \\ &+ \frac{RM_{22}e^{R^2/2}}{(2\pi\beta)^{1/2}(1 - m^2)^2} \int_0^{2\pi} \left[(\rho + k^2)P(k) + \frac{2k}{\sqrt{2\pi}} e^{-k^2/2} \right] \cdot \\ &\qquad \exp\left[-\frac{R^2(1 - mc)}{1 - m^2} \right] d\varphi \end{aligned} \tag{107}$$

which is the analogue of (57). When R becomes very large and τ small in such a way to keep $R\tau$ fixed, $p_1(\tau, R)$ approaches zero from physical considerations. We also have near $\varphi = 0$

$$\begin{aligned} &\frac{R^2}{2} - \frac{R^2(1 - mc)}{1 - m^2} \to -\frac{\beta R^2\tau^2}{8} - \frac{R^2\varphi^2}{2\beta\tau^2}, \\ &k \to R\beta B^{-1/2} - R\varphi^2\tau^{-2}B^{-1/2}. \end{aligned} \tag{108}$$

The first line in (108) shows that most of the contribution to the integral in (107) comes from the region where φ is $0(\tau/R)$. In this region, the second term in the approximation for k is negligible in comparison with the first, so k is large and positive and hence $P(k)$ is nearly unity. Thus when R is large (107) becomes

$$p_1^*(\tau, R) \rightarrow \frac{\beta\tau R^2}{4} e^{-R^2\tau^2\beta/8} \tag{109}$$

which is of the same form as (66). Therefore, as we might expect, the interval lengths for large values of R are distributed in much the same way as are the interval lengths of $I(t)$ for large values of I.

VIII. COMPUTATIONS

The computations for the curves shown in Figs. 1 and 2 were based on either the power spectrum (16) or (20), depending on whether $I(t)$ or $R(t)$ was being considered. In both cases the bandwidth parameter σ was taken to be $1/(2\pi)$, so that both β and β_r were unity and

$$m = \exp(-\tau^2/2). \tag{110}$$

This autocorrelation function was also used by Palmer[5] in his computations.

Fig. 7 shows curves of the first approximation $f_1(u, I)$ to the probability density $f(u, I)$ for the lengths of the intervals during which $I(t)$

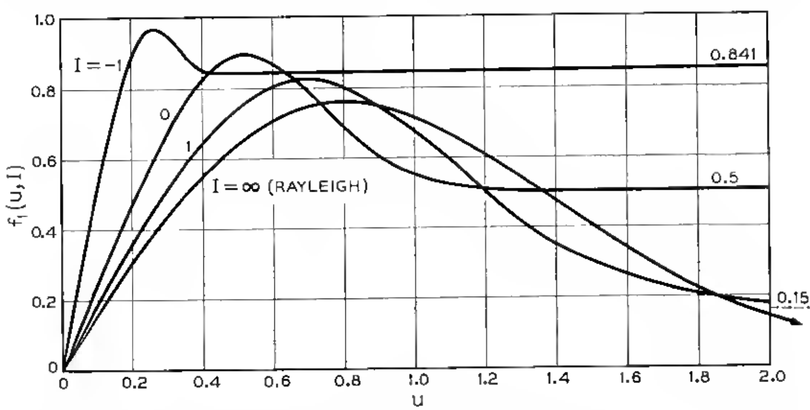

Fig. 7 — Graphs of the first approximation $f_1(u, I)$ when the power spectrum has the normal-law form (16). The rms value of $I(t)$ is one.

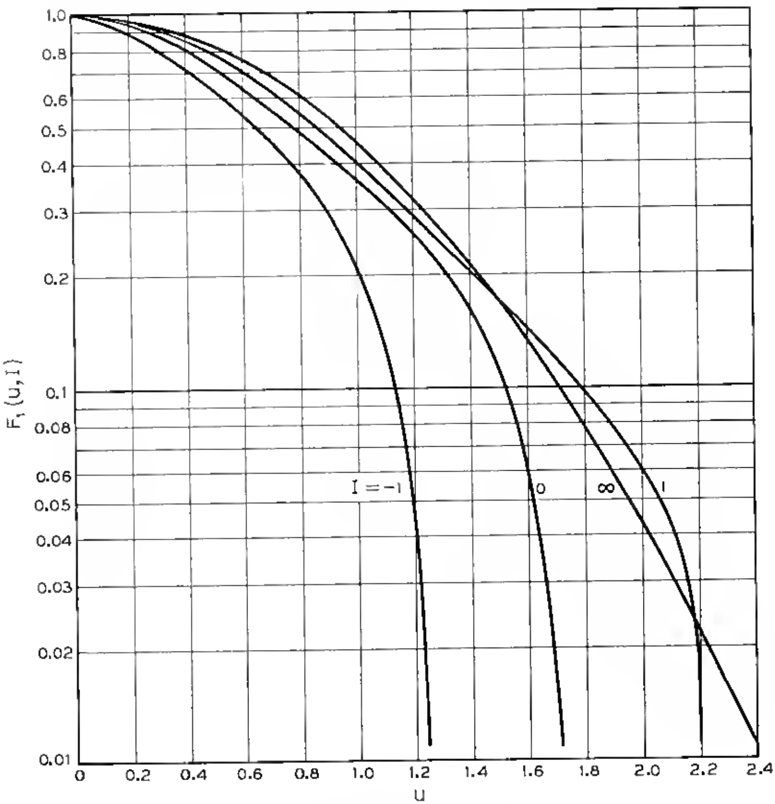

Fig. 8 — Graphs of the first approximation $F_1(u, I)$ to the interval length distribution $F(u, I)$. Estimates of $F(u, I)$ are shown in Fig. 1.

exceeds I. These curves were calculated from (47), (71) and tables[8] giving values of $K(r, h)$. Fig. 8 gives curves of $F_1(u, I)$ computed from $f_1(u, I)$ by means of (73). $F_1(u, I)$ is the first approximation to the cumulative distribution $F(u, I)$, estimates of which are shown in Fig. 1. One way of estimating $F(u, I)$ from $F_1(u, I)$ is to connect the $F_1(u, I)$ curve smoothly to a curve which approaches a straight line on the semi-log coordinates of Fig. 8, the slope and position of the straight line being chosen so as to make

$$\int_0^\infty F(u, I)\, du = 1. \tag{111}$$

This relation follows from the fact that the average value of u is unity. The linear behavior ensures that $F(u, I)$ decreases exponentially as u

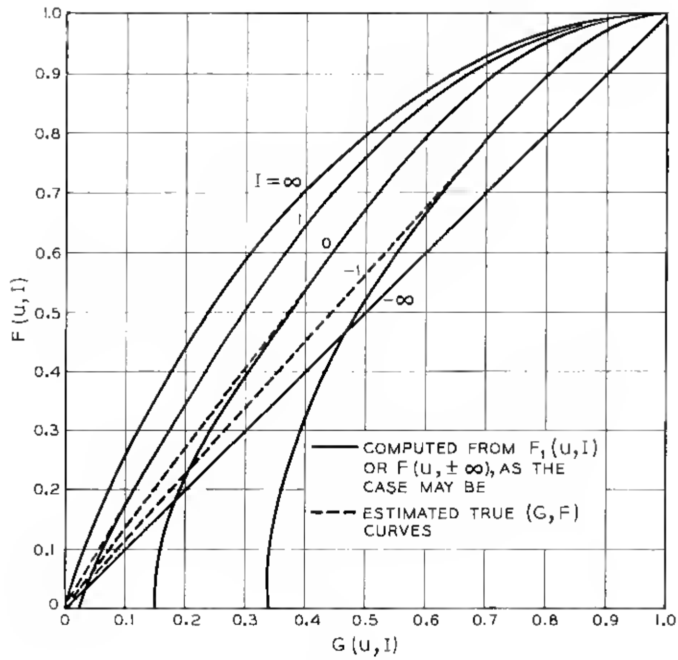

Fig. 9 — Graphs of (G_1, F_1) curves and estimates of the corresponding true (G, F) curves for $I(t)$.

becomes large. However, here $F(u, I)$ is estimated from $F_1(u, I)$ by the method outlined in Section VI. Fig. 9 shows (G, F) curves of the type illustrated in Fig. 6. The estimates of $F(u, I)$ given by Fig. 1 were obtained by connecting the curves of Fig. 9 to lines passing through the origin in a "smooth and reasonable" manner. The relation between u and $F(u, I)$ was determined by numerical integration from (75).

As a guide to what "smooth and reasonable" means, the case $I = 0$ was studied more completely with the help of the second approximation (83) and the computations made by Palmer[5] from his approximate integral equation. Some of this information is shown in Fig. 10. Palmer's results lead to a (G, F) curve (not shown) which lies slightly above the second approximation curve when G lies between 0.25 and 0.55. As G decreases below 0.25 the separation between the two curves increases and the curve from Palmer's results coincides with our estimate of the true (G, F) curve.

Fig. 11 shows curves of the first approximation $f_1(u, R)$ to the probability density $f(u, R)$ for the lengths of the intervals during which the

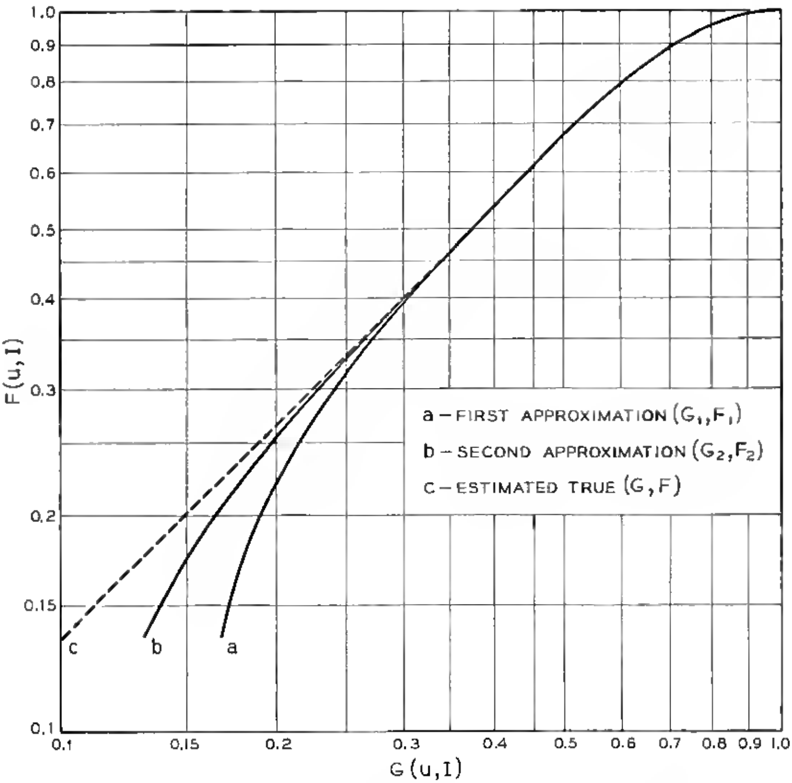

Fig. 10 — First and second approximation (G, F) curves for $I = 0$.

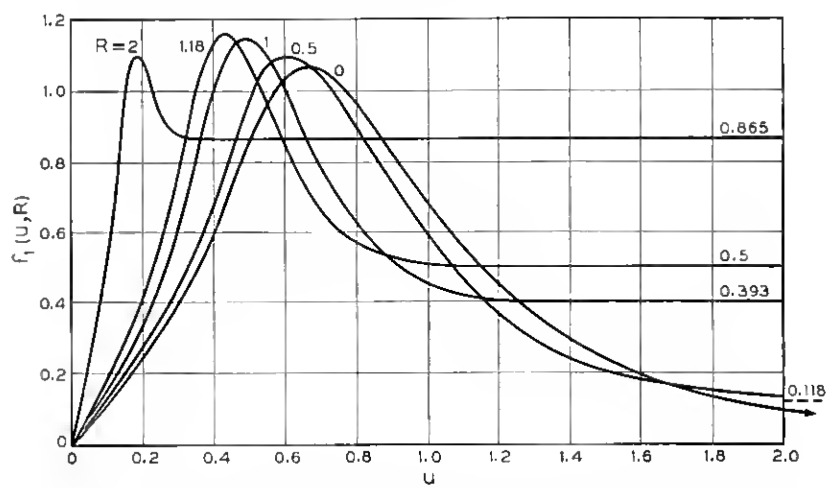

Fig. 11 — Graphs of the first approximation $f_1(u, R)$ when the power spectrum has the normal-law form (20). The median value of $R(t)$ is 1.18.

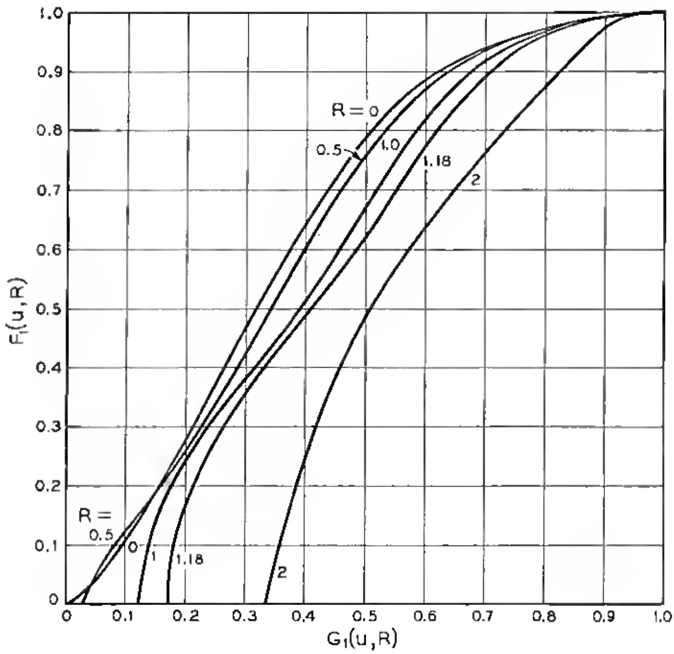

Fig. 12 — Graphs of the (G_1, F_1) curves for $R(t)$.

envelope $R(t)$ is less than R. These curves are the analogues of the curves for $I(t)$ shown in Fig. 7. Likewise, the (G, F) curves shown in Fig. 12 are the analogues of the curves of Fig. 9, and the estimates of $F_r(u, R)$ given in Table III were obtained from them. The functions $f_1(u, R)$, defined by (101), were computed by numerical integration from (97).

IX. COMMENTS ON A MARKOFF PROCESS

The foregoing work supposes that the autocorrelation function m of $I(t)$ is such that its second derivative with respect to τ exists at $\tau = 0$. This is not true when $w(f)$ has the form $4/[1 + (2\pi f)^2]$. In this case m is $\exp(-|\tau|)$ and m'' is infinite at $\tau = 0$. $I(t)$ is now a "Markoff process" and a formal calculation of the average distance between successive zeros gives $\bar{l} = 0$.

Although the distribution function for the intervals between zeros does not exist in the usual sense, some related information is available. Most of it is due to A. J. F. Siegert.[12] Here we shall list several of his

results and comment on their relation to the work of this paper.* For the sake of simplicity we take $\overline{I^2(t)} = 1$ and $m = \exp(-|\tau|)$.

1. The probability $W(I, \tau)\, d\tau$ that $I(t)$ reaches the value 0 for the first time between τ and $\tau + d\tau$ ("first passage time") starting from I at time $t = 0$ is

$$W(I, \tau)\, d\tau = (2/\pi)^{1/2} I \exp(-I^2 z^2/2)(-dz),$$

$$z = e^{-\tau}(1 - e^{-2\tau})^{-1/2}, \qquad -dz = e^{2\tau} z^3\, d\tau. \tag{112}$$

Wang and Uhlenbeck[13] obtained this result by solving an associated diffusion problem (by a method first used by Smoluchowski) in which the $I = 0$ axis corresponds to an absorbing barrier. Another derivation of (112) has been given by Siegert,[14] who obtains it as a solution of an integral equation.

2. The chance that $I(t)$ will go through zero for the first time in τ, $\tau + d\tau$ given that $I(0) > 0$ is

$$Q(\tau)\, d\tau = (2/\pi) e^{-\tau}(1 - e^{-2\tau})^{-1/2}\, d\tau. \tag{113}$$

By symmetry, the condition $I(0) > 0$ may be replaced by $I(0) \neq 0$. $Q(\tau)\, d\tau$ is also the probability that the interval between an instant selected at random and the next following zero of $I(t)$ has a length l lying between τ and $\tau + d\tau$.

3. The chance that l exceeds τ seconds is

$$\int_\tau^\infty Q(t)\, dt = \frac{2}{\pi} \sin^{-1} e^{-\tau} \tag{114}$$

where the arc lies between 0 and $\pi/2$.

4. Let $I(t)$ be observed over a long period of time T. The expected number of spacings between successive zeros whose lengths exceed τ seconds is

$$N_T(\tau) = Q(\tau) T. \tag{115}$$

Furthermore, the probability that an instant selected at random will fall in a space whose length exceeds τ is

$$\tau Q(\tau) + (2/\pi) \sin^{-1} e^{-\tau}. \tag{116}$$

Items 2, 3, and 4 are due to Siegert[12] and were obtained by analysis similar to that given in his paper.[14] David Slepian has pointed out, in

* I am indebted to Mr. Siegert for a copy of his report, which contains the results listed here.

some unpublished work, that (114) may also be obtained from the probability

$$P_{++} = \frac{1}{4} + \frac{1}{2\pi} \sin^{-1} e^{-\tau} \tag{117}$$

that both $I(0)$ and $I(\tau)$ be positive. His derivation runs as follows. The probability (114) is twice the probability that $I(t)$ be positive over an interval of length τ selected at random. This last probability is $P_{++} - P_{+0+}$ where P_{+0+} is the chance that $I(0) > 0$, $I(\tau) > 0$ and $I(t)$ is zero at one or more points in $0 < t < \tau$. Since the process is Markoffian and symmetrical about zero, consideration of the behavior of $I(t)$ between its first zero (if it has one) and τ shows that P_{+0+} is equal to P_{+0-}, i.e. to P_{+-}. The sum of P_{++} and P_{+-} is the probability that $I(0)$ be positive, which is $\frac{1}{2}$. We then have

$$2(P_{++} - P_{+0+}) = 2(P_{++} - P_{+-}) = 4P_{++} - 1 = \frac{2}{\pi} \sin^{-1} e^{-\tau}$$

and this gives (114). The expression (117) for P_{++} is readily obtained by integrating the joint probability density.

5. It should be possible to obtain (114) by letting n approach infinity in the expression for two times the probability that $I(0)$, $I(\tau/n)$, $\cdots$, $I(n\tau/n)$ all be positive. The expression which should approach (114) is

$$\begin{aligned} &2\pi^{-(n+1)/2}(1 - \alpha^2)^{1/2} \int_0^\infty dx_1 \cdots \int_0^\infty dx_{n+1} \cdot \\ &\qquad \exp [- x_1^2 - x_{n+1}^2 - (1 + \alpha^2)(x_2^2 + \cdots + x_n^2) \\ &\qquad\qquad + 2\alpha(x_1 x_2 + x_2 x_3 + \cdots + x_n x_{n+1})] \end{aligned} \tag{118}$$

where α denotes $\exp(-\tau/n)$.

This method of obtaining (114) is appealing because of its directness. Unfortunately, it seems that no one has yet succeeded in carrying out the limiting process. Some idea of how the limit is approached may be obtained from Table IV.

The values shown in the columns for $n = 1$ and $n = 2$ were computed from the corresponding known expressions for (118), namely

$$1 - \frac{1}{\pi} \cos^{-1} e^{-\tau} = 2P_{++},$$

$$1 - (\tfrac{1}{2\pi})(2 \cos^{-1} e^{-\tau/2} + \cos^{-1} e^{-\tau}).$$

When τ is small these behave like $1 - 0.45\sqrt{\tau}$ and $1 - 0.54\sqrt{\tau}$

TABLE IV — VALUES OF EXPRESSIONS (118) AND (114)

Value of (118)						Value of (114)
τ	$e^{-\tau}$	$n = 1$	$n = 2$	$n = 3$	$n = 4$	
0	1	1	1	1	1	1
0.05	0.951	0.900	0.879	0.868	0.861	0.800
0.10	0.905	0.860	0.830	0.814	0.804	0.720
0.15	0.861	0.830	0.793	0.774	0.761	0.660
0.20	0.819	0.805	0.763	0.742	0.726	0.611
0.40	0.670	0.734	0.672	0.641	0.620	0.474
∞	0	0.500	0.250	0.125	0.0625	0

respectively, while (114) becomes $1 - 0.90\sqrt{\tau}$. When $n = 4$ the five-fold integral may be reduced to

$$2\pi^{-1/2}(1 - \alpha^2)^{1/2} \int_0^\infty dx_3[K(r, -h, -k)]^2 \exp\,[-(1 - \alpha^2)x_3^2] \quad (119)$$

where $K(r, h, k)$ is the d/N tabulated in Ref. 8, and

$$r = \alpha(1 + \alpha^2)^{-1/2}, \qquad h = 2^{1/2}\alpha x_3\,, \qquad k = rh.$$

When α is near unity it is helpful to set

$$K(r, -h, -k) = 1 - L,$$

$$L = 1 - K(r, h, k) - \tfrac{1}{2}P(h) - \tfrac{1}{2}P(k).$$

The contribution of the 1 in $1 - 2L + L^2$ to (119) is unity and the contribution of $-2L + L^2$ may be obtained by numerical integration. Replacing the square of $K(r, -h, -k)$ in (119) by

$$K(r, -h, -k)[1 + P(h)]/2$$

gives an expression for (118) when $n = 3$.

6. The probabilities stated in Items 2, 3, and 4 have already appeared in Section VI for the well-behaved cases in which $\bar{t}$ exists. Thus, from (79) the analogue of $Q(\tau)\,d\tau$ is $P(\tau, I)\,d\tau/\bar{t}$, or $F(u, I)\,du$, and the analogue of (114) is $G(u, I)$. The probability (81) that a point chosen at random falls in an interval longer than τ goes into the corresponding expression (116).

These analogies lead us to regard $Q(\tau)$ and its integral (114) as being irregular versions of F and G (with τ playing the role of u) for which a (G, F) curve may be plotted with the help of expressions (113) and (114). When this is done, it is seen that F approaches infinity as G approaches unity. However, the other parts of the curve behave in much the same manner as in the earlier cases.

X. ACKNOWLEDGMENT

I wish to express my thanks to a number of my associates for their helpful remarks and for references to pertinent material. I am especially indebted to A. L. Durkee and D. Slepian for discussions on the contents of Sections IV and IX, respectively, and to Miss Katherine Jillson for computing the various tables and curves.

APPENDIX I

Minors of the Determinant M

Here we list the values of the minors of the determinant M defined by equation (40) and state some of the relations between them.

$$\begin{aligned}
M_{11} &= M_{44} = \beta^2 - m''^2 - \beta m'^2, \\
-M_{12} &= M_{34} = m'm'' + mm'\beta, \\
M_{13} &= -M_{24} = m'^3 - m'\beta - mm'm'', \\
M_{22} &= M_{33} = \beta(1 - m^2) - m'^2, \\
M_{14} &= mm''^2 - m\beta^2 - m'^2 m'', \\
M_{23} &= m''(1 - m^2) + mm'^2,
\end{aligned} \tag{120}$$

$$M = [(\beta + m'')(1 + m) - m'^2][(\beta - m'')(1 - m) - m'^2], \tag{121}$$

$$\begin{aligned}
\frac{M_{11} + M_{14}}{\beta + m''} = \frac{M_{12} + M_{24}}{m'} &= \frac{M_{22} - M_{23}}{1 + m} \\
&= (\beta - m'')(1 - m) - m'^2
\end{aligned} \tag{122}$$

$$\begin{aligned}
M_{22} + M_{23} &= (1 - m)[(\beta + m'')(1 + m) - m'^2] \\
M &= (M_{11} + M_{14})(1 + m) - m'(M_{12} + M_{24}).
\end{aligned}$$

We also have relations of the form

$$\begin{aligned}
M_{22}^2 - M_{23}^2 = \begin{vmatrix} M_{22} & M_{23} \\ M_{32} & M_{33} \end{vmatrix} &= (-)^{2+2+3+3} \begin{vmatrix} 1 & m \\ m & 1 \end{vmatrix} M \\
&= (1 - m^2)M, \\
M_{12}M_{22} + M_{23}M_{24} = \begin{vmatrix} M_{12} & M_{13} \\ M_{32} & M_{33} \end{vmatrix} &= (-)^{1+2+3+3} \begin{vmatrix} 0 & -m' \\ m & 1 \end{vmatrix} M \\
&= -m'mM,
\end{aligned} \tag{123}$$

$$M_{23}M_{12} + M_{22}M_{24} = m'M,$$
$$M_{11}M_{33} - M_{13}^2 = (\beta - m'^2)M,$$
$$M_{14}M_{23} + M_{13}^2 = (m'^2 - mm'')M,$$
$$M_{11}M_{23} + M_{14}M_{22} = (m'' - \beta m)M.$$

APPENDIX II

Expressions for Various Parameters When τ Becomes Small

In dealing with $I(t)$ we shall put

$$b_{2n} = (2\pi)^{2n} \int_0^\infty w(f) f^{2n}\, df, \qquad n = 0, 1, 2, \cdots \tag{124}$$

and in particular

$$\begin{aligned} &b_0 = 1, \qquad b_2 = \beta, \qquad b_4 = \gamma, \\ &B = b_4 - b_2^2 = \gamma - \beta^2, \\ &C = b_2 b_6 - b_4^2 = \beta b_6 - \gamma^2. \end{aligned} \tag{125}$$

The results for $I(t)$ may be carried over directly into those for the envelope $R(t)$ of a narrow-band noise current whose power spectrum is symmetrical about the midband frequency f_0. This is accomplished by replacing the definition (124) for b_{2n} by

$$b_{2n} = (2\pi)^{2n} \int_0^\infty w(f)(f - f_0)^{2n}\, df. \tag{126}$$

For the normal-law power spectrum used in our computations γ is equal to $3\beta^2$ and B becomes $2\beta^2$.

It follows from (41) that when τ is small and the b's exist,

$$\begin{aligned} m &= 1 - \frac{\beta\tau^2}{2!} + \frac{\gamma\tau^4}{4!} - \frac{b_6\tau^6}{6!} + \cdots, \\ m' &= -\beta\tau + \cdots, \\ m'' &= = -\beta + \cdots. \end{aligned} \tag{127}$$

These expansions may be used to show that

$$
\begin{aligned}
1 - m &\to \frac{\beta\tau^2}{2}, \\
1 + m &\to 2 - \frac{\beta\tau^2}{2}, \\
1 - m^2 &\to \beta\tau^2 - \cdots, \\
(\beta + m'')(1 + m) - m'^2 &\to \tau^2 B, \\
(\beta - m'')(1 - m) - m'^2 &\to \tau^6 C/144, \\
M_{23} \to M_{22} &\to \tau^4 \beta B/4, \\
M_{22} - M_{23} &\to \tau^6 C/72, \\
M &\to \tau^8 BC/144, \\
M_{22}^2 - M_{23}^2 &\to \tau^{10}\beta BC/144, \\
(1 - m^2)/M_{22} &\to 4/B\tau^2.
\end{aligned}
\tag{128}
$$

APPENDIX III

An Approximation to the Cumulative Probability $P(\tau, I)$

In Section V we worked with a first approximation $p_1(\tau, I)$ to the probability density $p(\tau, I)$ for the lengths of the $I(t) > I$ intervals. Here we note a rather simple approximation $P_1(\tau, I)$ to the probability $P(\tau, I)$ that an interval selected at random from the universe of $I(t) > I$ intervals will be longer than τ. We take $P_1(\tau, I)$ to be the limit, as dt approaches zero, of a fraction having the numerator

[Probability that $I(\tau) > I$ given that $I(t)$ passes upward through the value I during the interval $(0, dt)$]

and the denominator

[Probability $I(t)$ passes upward through I in $(0, dt)$].

By proceeding as in Section V it may be shown that

$$P_1(\tau, I) = \frac{1}{2} - \frac{1}{2} P\left(\frac{k}{s}\right) + \frac{r}{2}\left[1 + P\left(\frac{rk}{s}\right)\right] \exp\left(-k^2/2\right) \tag{129}$$

where $P(x)$ is the error integral (3), and now

$$r = -m'\beta^{-1/2}(1 - m^2)^{-1/2}, \qquad s^2 = 1 - r^2,$$
$$k = I[(1 - m)/(1 + m)]^{1/2},$$

with m and β the same as in Section V. The approximation given by $P_1(u\bar{t}, I)$ to $F(u, I)$ is not as good as the $F_1(u, I)$ given by (73) (which is based on the $p_1(\tau, I)$ of Section V), but we do have $P_1(u\bar{t}, I) \geqq F(u, I) \geqq F_1(u, I)$. This may lead to another proof of (66).

APPENDIX IV

Fade Length Distributions Having a Large Percentage of Long Fades

Some, but not all, of the small number of available experimental observations of fade lengths show a greater percentage of long fades than those shown in Figs. 2 and 3. Since our calculations are based on a normal-law power spectrum, it is of interest to know whether a different power spectrum may give a larger percentage of long fades. An example of such a power spectrum is studied in the first part of this appendix. The second part is concerned with a guess as to how the very long fades are distributed.

The power spectrum

$$w(f) = \frac{4}{1 + (2\pi f)^2}, \tag{130}$$

which has been discussed in Section IX, is quite different from the normal-law type. The power carried by the high frequencies in this spectrum is so large that $\bar{t} = 0$, and our method of investigating interval lengths breaks down. Our formulas will still apply, though, if the high frequencies are attenuated by some factor such as $a^4/[a^2 + (2\pi f)^2]^2$. An attenuation of this type might either exist in nature or be produced by the measuring apparatus. Here we shall take

$$w(f) = \frac{8a^3(a + 1)^2/(2a + 1)}{[1 + (2\pi f)^2][a^2 + (2\pi f)^2]^2} \tag{131}$$

where the numerator has been chosen so as to make the integral of $w(f)$ from 0 to ∞ equal to unity.

If it were not for the considerable amount of additional work required, we would investigate the interval length distribution associated with the envelope of an $I(t)$ having the power spectrum obtained from (131) by setting $(f - f_0)$ in place of f and changing the 8 in the numerator to

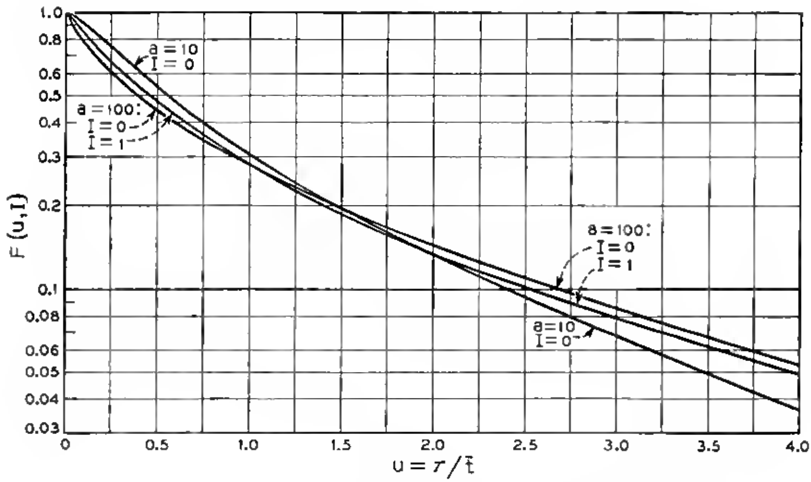

Fig. 13 — The probability $F(u, I)$ that $I(t) > I$ for an interval lasting longer than τ. $I(t)$ has the power spectrum given by equation (131) and $\bar{t}_0$ is $\pi a^{-1}\sqrt{2a+1}$.

4. Instead, we shall apply the results of Section V to obtain the interval length distribution associated with an $I(t)$ having the power spectrum (131), and rely on the similarity between the curves of Figs. 1 and 2.

The general theory of Section VII shows that, as R approaches 0, the fade length distribution $F_r(u, R)$ of the envelope approaches the form $F_r(u, R \to 0)$ shown in Fig. 4. However, when a is very large it appears that this limiting form will have to be approached by going through shapes similar to those shown in Fig. 13. This indicates that the values of R will have to be very small indeed before $F_r(u, R)$ begins to look like the $F_r(u, R \to 0)$ of Fig. 4.

The autocorrelation function m, defined by (41), and its derivatives with respect to τ are, assuming $\tau > 0$,

$$\begin{aligned} m &= x - y[3a^2 - 1 + a\tau(a^2 - 1)], \\ m' &= -x + ya[2a^2 + a\tau(a^2 - 1)], \\ m'' &= x - ya^2[a^2 + 1 + a\tau(a^2 - 1)], \end{aligned} \tag{132}$$

where

$$\begin{aligned} x &= 2Aa^3 e^{-\tau}, \qquad y = A\, e^{-a\tau}, \\ A &= 1/(2a + 1)(a - 1)^2. \end{aligned} \tag{133}$$

The expansion of m in powers of τ up to the fifth is

$$m = 1 - \frac{\beta\tau^2}{2!} + \frac{\gamma\tau^4}{4!} - \frac{a^3 \mid \tau \mid^5}{5!} \frac{2(a + 1)^2}{2a + 1}, \tag{134}$$

in which

$$\begin{gathered}\beta = a^2/(2a + 1), \qquad \gamma = a^3(a + 2)/(2a + 1), \\ B = \gamma - \beta^2 = 2a^3(a + 1)^2/(2a + 1)^2.\end{gathered} \tag{135}$$

From β and γ it follows that the average interval between the zeros of $I(t)$ is $\pi a^{-1}\sqrt{2a + 1}$, and the expected number of maxima per second is $(2\pi)^{-1}\sqrt{a(a + 2)}$.

These expressions were used to compute $p_I(\tau, I)$ from (47), and the method outlined in Section VI was applied to obtain the curves shown in Fig. 13. These curves are for $a = 10$ and $a = 100$. Difficulty was encountered, in the $a = 100$ case, in extrapolating the distributions for small values of τ to obtain $F(u, I)$ for the larger values of u. Consequently, these curves are not too reliable, but there seems to be enough truth in them to show that the percentage of long fades is larger than for the distributions of Fig. 1 pertaining to the normal-law power spectrum.

Irrespective of whether power spectra of the form (131) have any practical significance, it is interesting to speculate on how the corresponding interval length distribution $F(u, I)$ behaves for large values of u. When a becomes large, $I(t)$ has many more maxima than zeros (the average number of maxima between successive zeros approaches $\sqrt{a/2}$), and we are led to picture the power spectrum (131) as consisting of two parts.

One part is the "low-frequency" portion which behaves like (130) and extends from zero up to a frequency at which the cutoff factor begins to operate. The other, the high-frequency portion, extends from this frequency to infinity. Most of the power is in the low-frequency part and we may regard it as producing most of the deviation of $I(t)$ from zero. The high-frequency part produces small rapid fluctuations which are superposed on the more slowly changing low-frequency portion of $I(t)$. Thus the high-frequency part produces the large number of maxima and the low-frequency part controls the drift towards or away from the value $I(t) = 0$. According to this picture some relation might be expected between $F(u, 0)$ and $Q(\tau)$ [given by (113)] when u is large. In fact, comparison of (79) and (113) suggests that $F(u, 0)\, du$ approaches $Q(\tau)\, d\tau$ for the larger values of τ:

$$F(u, 0) \to \bar{t}(2/\pi)e^{-\tau}(1 - e^{-2\tau})^{-1/2}, \qquad \tau = u\bar{t}. \tag{136}$$

The curves shown in Fig. 13 indicate that (136) may not hold when $a = 10$, but may do so when $a = 100$. Evidently, if (136) is to be valid, it is necessary that the number of maxima between zeros be large. This is

also suggested by the original derivation of (112), which is based upon an analogy with the Brownian motion of a particle subject to an elastic force.

If the relation (136) between $F(u, 0)$ and $Q(\tau)$ should turn out to be true, it would be helpful to have expressions for the generalizations $Q(\tau, I)$ and $Q_r(\tau, R)$ of $Q(\tau)$ corresponding to the "first passage times" down through the level $I(t) = I$ and up through the level $R(t) = R$, respectively. These generalizations may be obtained by the method used by Wang and Uhlenbeck mentioned in Item 1 of Section IX. The derivations are sketched in the following paragraphs.

Let $I(t)$ have the power spectrum (130) and let $W(I, I_1, \tau)d\tau$ be the probability that $I(t)$ passes down through the level I for the first time in the interval $\tau, \tau + d\tau$ when it starts from the level I_1, which is greater than I, at time $t = 0$. Then $W(I, I_1, \tau)\, d\tau$ is equal to $(\partial P/\partial x)\, d\tau$ evaluated at $x = I$ and $t = \tau$, where P is the solution of the diffusion equation

$$\frac{\partial P}{\partial t} = \frac{\partial^2 P}{\partial x^2} + x\frac{\partial P}{\partial x} + P \tag{137}$$

which is zero at $x = I$ for all time and is concentrated around $x = I_1$ at time 0 [i.e., equals $\delta(x - I_1)$ at time $t = 0$]. The probability $Q(\tau, I)\, d\tau$ that if $I(0) > I$ then $I(t)$ passes down through the level I for the first time in $\tau, \tau + d\tau$ is obtained from

$$Q(\tau, I) = \int_I^\infty \frac{\exp(-I_1^2/2)}{\sqrt{2\pi}} W(I, I_1, \tau)\, dI_1/\mathrm{prob}[I(0) > I]. \tag{138}$$

A typical solution of (137) is

$$e^{-x^2/4} D_n(x)\, e^{-nt} \tag{139}$$

where $D_n(x)$ is the parabolic cylinder function. The boundary condition at $x = I$ gives the equation

$$D_n(I) = 0 \tag{140}$$

to determine the eigenvalues n_i, $i = 1, 2, \cdots$. A formal application of the Sturm-Liouville theory shows that P may be expressed as a sum of terms of the type (139), with suitable coefficients, when n is replaced by n_i and the summation taken over i. If the typical eigenfunction is denoted by $a_i D_{n_i}(x)$, the relation to determine the normalizing constant a_i is obtained by differentiating

$$(n - n_i)\int_I^\infty D_n(x) D_{n_i}(x)\, dx = -D_n(I) D_{n_i}'(I) \tag{141}$$

with respect to n and then setting $n = n_i$. In (141), which may be obtained from the differential equation for $D_n(x)$, we have denoted $\partial D_n(x)/\partial x$ by $D_n'(x)$.

It is found that

$$W(I, I_1, \tau) = \exp[(I_1^2 - I^2)/4] \sum_{i=1}^{\infty} a_i^2 D_{n_i}(I_1) D_{n_i}'(I)\, e^{-n_i\tau}, \quad (142)$$

$$Q(\tau, I) = \frac{(2\pi)^{-1/2}\, e^{-I^2/2}}{2^{-1}[1 - P(I)]} \sum_{i=1}^{\infty} \frac{D_{n_i}'(I)\, e^{-n_i\tau}}{n_i[-\partial D_n(I)/\partial n]_{n=n_i}}, \quad (143)$$

where $P(I)$ is the error integral (3) and

$$a_i^{-2} = D_{n_i}'(I)\,[-\partial D_n(I)/\partial n]_{n=n_i}. \quad (144)$$

The integration (138) used to obtain (143) from (142) makes use of a result obtained by integrating a form of the differential equation for $D_n(x)$.

Siegert's result (115) now reads as follows: When $I(t)$ is observed over a long period of time T, the expected number of $I(t) > I$ intervals whose lengths exceed τ seconds is

$$N_T(\tau, I) = \frac{T}{2}\,[1 - P(I)]Q(\tau, I). \quad (145)$$

This may be seen by writing (79) as

$$\frac{N_T(\tau, I)\, d\tau}{T \text{ prob } \{I(t) > I\}} = Q(\tau, I)\, d\tau.$$

When $I = 0$, the values of the n_i are $1, 3, 5, \cdots$ and it may be shown that (143) reduces to (113) as it should. As I becomes large and positive the n_i's increase in value, so that $n_1 \approx I^2/4$ and the first few succeeding n_i's differ from n_1 by terms of order $I^{2/3}$. Furthermore, setting $n = n_i$ and approximating $D_{n-1}(I)$ by $(-1)\ \partial D_n(I)/\partial n$ in the relation

$$D_n'(I) + \frac{I}{2} D_n(I) - nD_{n-1}(I) = 0$$

suggests that when I is large and i not too large

$$D_{n_i}'(I)/n_i[-\partial D_n(I)/\partial n]_{n_i} \approx 1,$$

and hence we may expect $Q(\tau, I)$ to be of the form of $I \exp(-I^2\tau/4)$ times a more slowly varying function of τ and I.

In much the same way, expressions may be derived for $W_r(R, R_1, \tau)$ and $Q_r(\tau, R)$ corresponding to the envelope $R(t)$ of a Gaussian noise

current $I(t)$ whose power spectrum is obtained from (130) by substituting $f - f_0$ for f and replacing the 4 in the numerator by 2. Instead of (137) we must use

$$\frac{\partial P}{\partial t} = \frac{\partial^2 P}{\partial r^2} + \left(r - \frac{1}{r}\right)\frac{\partial P}{\partial r} + \left(1 + \frac{1}{r^2}\right)P \tag{146}$$

where $P = 2\pi r\, P_x P_y$ now is the probability density or concentration corresponding to a narrow circular ring of radius $r = \sqrt{x^2 + y^2}$ and P_x, P_y are, respectively, solutions of (137) and the corresponding equation in y.

The probability $W_r(R, R_1, \tau)\, d\tau$ that the envelope $R(t)$ passes up through the value R for the first time in τ, $\tau + d\tau$ when it starts from R_1, less than R, at time $t = 0$ is $-(\partial P/\partial r)\, d\tau$ evaluated at $r = R$ and $t = \tau$. Here P is the solution of (146) which is zero at the boundary $r = R$ for all t and is $\delta(r - R_1)$ at time $t = 0$.

The typical solution of (146) is

$$r^{1/2} e^{-r^2/4} v(\alpha, r)\, e^{-\alpha t} \tag{147}$$

where α is a parameter similar to n in the earlier case, and

$$v(\alpha, r) = r^{1/2}\, e^{-r^2/4}\, {}_1F_1\left(-\frac{\alpha}{2}; 1; \frac{r^2}{2}\right) \tag{148}$$

becomes the typical orthogonal function for the range $0 \leqq r \leqq R$ when α is one of the roots α_i, $i = 1, 2, 3, \cdots$ of the equation

$${}_1F_1\left(-\frac{\alpha}{2}; 1; \frac{R^2}{2}\right) = 0. \tag{149}$$

For very large values of R, α_i approaches $0, 2, 4, \cdots$ and the confluent hypergeometric function in (148) becomes the Laguerre polynomial $L_{i-1}(r^2/2)$. For very small values of R, $v(\alpha_i, r)$ approaches

$$\sqrt{r}\, J_0(r\sqrt{\alpha_i + 1})$$

and $R\sqrt{\alpha_i + 1}$ becomes the ith root of the Bessel function $J_0(x)$. Some rough work indicates that α_1 is approximately 5 for $R = 1$ and 3.25 for $R = 1.18$. When R is very small $\alpha_1 + 1$ is approximately $5.78/R^2$.

It is found that

$$P = (r/R_1)^{1/2} \exp\left[(R_1^2 - r^2)/4\right] \sum_{i=1}^{\infty} a_i^2 v(\alpha_i, R_1) v(\alpha_i, r)\, e^{-\alpha_i t} \tag{150}$$

where the normalizing constant a_i is given by

$$a_i^2 \left[\frac{\partial v(\alpha, R)}{\partial \alpha} \right]_{\alpha=\alpha_i} \left[\frac{\partial v(\alpha_i, r)}{\partial r} \right]_{r=R} = 1.$$

When the expression for $W_r(R, R_1, \tau)$ obtained by differentiating P is set in the equation corresponding to (138), we obtain

$$Q_r(\tau, R) = \frac{R}{\exp [R^2/2] - 1} \sum_{i=1}^{\infty} \frac{e^{-\alpha_i \tau}}{\alpha_i} \frac{[\partial v(\alpha_i, R)/\partial R]}{[\partial v(\alpha, \quad R)/\partial \alpha]_{\alpha=\alpha_i}} \tag{151}$$

where $Q_r(\tau, R)\, d\tau$ is the probability that $R(t)$ will pass up through the level R for tbe first time in τ, $\tau + d\tau$, given tbat $R(0) < R$.

In the limit as R becomes small, (151) reduces to

$$Q_r(\tau, R) \to 4R^{-2} \sum_{i=1}^{\infty} e^{-\alpha_i \tau}, \tag{152}$$

$$R\sqrt{\alpha_i} \to [i\text{tb root of } J_0(x)].$$

When (152) is integrated with respect to τ between the limits 0 and ∞ the result is 1, as it should be. The result (152) bas probably been given before, since it is closely related to Brownian motion of a particle and to the first passage time across a circle, but a suitable reference has not been found by the author.

When R is small so that prob $[R(t) < R] \to R^2/2$, the relation (152) and the analogue of (145) for $R(t)$ lead to

$$N_T(\tau, R) \to 2T \sum_{i=1}^{\infty} e^{-\alpha_i \tau} \tag{153}$$

for the expected number, in the long time T, of $R(t) < R$ intervals whose lengths exceed τ seconds.

All of the discussion between equations (136) and (153) pertains to the power spectrum (130) or its analogue for $R(t)$. In tbe comparison of theory and experiment given in Section IV, it is convenient to deal instead with

$$w(f) = \frac{4k}{k^2 + (2\pi f)^2}. \tag{154}$$

The analogue of (154) for $R(t)$ has already appeared as equation (24). Results for (154) pertaining to duration of intervals, time averages and so on may be obtained from the corresponding results for (130) by replacing t by kt. Thus, for example, the probability $Q_r(\tau, R)\, d\tau$ goes into

$kQ_r(k\tau, R)\, d\tau$ and the number of $R(t) < R$ intervals longer than τ to be expected in time T, when R is small, is

$$N_T(\tau, R) \to 2kT \sum_{i=1}^{\infty} e^{-\alpha_i k\tau}, \tag{155}$$

where α_i is still given by the second relation in (152). Siegert's expression (115) for the expected number of spacings between successive zeros whose lengths exceed τ seconds is now

$$N_T(\tau) = (2kT/\pi)\, e^{-k\tau}(1 - e^{-2k\tau})^{-1/2}.$$

Incidentally, this may possibly lead to an estimate of k when one is trying to measure a power spectrum which insists on increasing as $1/f^2$ at the lowest frequencies which can be conveniently measured. The problem of estimating k from $N_T(\tau)$ has been discussed by Siegert.[12]

If the "low-frequency" portion of a power spectrum behaves like (154) instead of (130) the remarks in the preceding paragraph show that the analogue of (136) is

$$F(u, 0) \to k\bar{t}(2/\pi)\, e^{-k\tau}(1 - e^{-2k\tau})^{-1/2} \tag{156}$$

where $u = \tau/\bar{t}$ is assumed to be very large. The analogous surmise for $F_r(u, R)$ is that

$$F_r(u, R) \to k\bar{t}Q_r(k\tau, R) \tag{157}$$

where the low-frequency behavior of the power spectrum is given by (24). When R is small, this and (152) suggest that

$$F_r(u, R) \to 4k\bar{t}R^{-2} \sum_{i=1}^{\infty} e^{-\alpha_i k\tau} \tag{158}$$

for the probability that a long fade below the level R will last longer than τ seconds. Multiplying both sides of (158) by N_R and using

$$N_R\bar{t} = \text{prob}\,[R(t) < R] \to R^2/2$$

shows that the expected number of fades below level R, in unit time, whose lengths exceed τ is

$$N_R F_r(u, R) \to 2k \sum_{i=1}^{\infty} e^{-\alpha_i k\tau} \tag{159}$$

where α_i is related to the zeros of $J_0(x)$ as indicated by (152). The relation (159) is to be expected in view of (155).

REFERENCES

1. Bullington, K., Inkster, W. J. and Durkee, A. L., Results of Propagation Tests at 505 mc and at 4090 mc on Beyond-Horizon Paths, Proc. I.R.E., **43**, October, 1955, pp. 1306–1316.
2. Rice, S. O., Mathematical Analysis of Random Noise, B.S.T.J., **24**, January, 1945, pp. 46–156.
3. Rice, S. O., Statistical Properties of a Sine Wave Plus Random Noise, B.S.T.J., **27**, January, 1948, pp. 109–157.
4. Norton, K. A., Rice, P. L., Janes, H. B. and Barsis, A. P., The Rate of Fading in Propagation Through a Turbulent Atmosphere, Proc. I.R.E., **43**, October, 1955, pp. 1341–1353; Norton, K. A., Vogler, L. E., Mansfield, W. V. and Short, P. J., The Probability Distribution of the Amplitude of a Constant Vector Plus a Rayleigh-Distributed Vector, Proc. I.R.E., **43**, October, 1955, pp. 1354–1361.
5. Palmer, D. S., Properties of Random Functions, Proc. Cambridge Phil. Soc., **52**, October, 1956, pp. 672–686.
6. Favreau, R. R., Low, H and Pfeffer, I., Evaluation of Complex Statistical Functions by an Analogue Computer, presented at the 1956 I.R.E. Convention. An abstract appears in Proc. I.R.E., **44**, March, 1956, p. 388.
7. McFadden, J. A., The Axis-Crossing Intervals of Random Functions, I.R.E. Trans. on Information Theory, **IT-2**, December, 1956, p. 146; also a paper scheduled for the March 1958 issue of Trans. on Information Theory.
8. Pearson, Karl, ed., *Tables for Statisticians and Biometricians*, Cambridge Univ. Press, 1931, Part II, Table VIII, Volumes of Normal Bivariate Surface, pp. 78–109.
9. Kuznetsov, Stratonovich and Tikhonov, On the Duration of Exceedances of a Random Function, Journal of Technical Physics, **24**, 1954. Translated from the Russian by Goodman, N. R., New York Univ. Coll. of Engineering, Scientific Paper No. 5, Engineering Statistics Group, March, 1956.
10. Palm, Conny, *Intensitätsschwankungen im Fernsprechverkehr*, Ericsson Technics 44, L. M. Ericsson, Stockholm, 1943.
11. Ehrenfeld, S. and Goodman, R., private communication.
12. Siegert, A. J. F., On the Roots of Markoffian Random Functions, Rand memorandum, September 5, 1950.
13. Wang, Ming Chen and Uhlenbeck, G. E., On the Theory of the Brownian Motion II, Revs. Modern Phys., **17**, April—July, 1945, p. 323.
14. Siegert, A. J. F., On the First Passage Time Probability Problem, Phys. Rev., **81**, February 15, 1951, pp. 617–623.